nature nanotechnology

Article

https://doi.org/10.1038/s41565-024-01680-8

Bone-marrow-homing lipid nanoparticles for genome editing in diseased and malignant haematopoietic stem cells

In the format provided by the authors and unedited

Bone Marrow Homing Lipid Nanoparticles for Genome Editing in Diseased and Malignant Hematopoietic Stem Cells

Xizhen Lian,[1] Sumanta Chatterjee,[1] Yehui Sun,[1] Sean A. Dilliard,[1] Stephen Moore,[1] Yufen Xiao,[1] Xiaoyan Bian,[1] Kohki Yamada,[1] Yun-Chieh Sung,[1] Rachel M. Levine,[2] Kalin Mayberry,[2] Samuel John,[3] Xiaoye Liu,[3] Caroline Smith,[3] Lindsay T. Johnson,[1] Xu Wang,[1] Cheng Cheng Zhang,[3] David R. Liu,[4,5,6] Gregory A. Newby,[7] Mitchell J. Weiss,[2] Jonathan S. Yen,[2] and Daniel J. Siegwart[1,*]

[1]Department of Biomedical Engineering, Department of Biochemistry, Simmons Comprehensive Cancer Center, Program in Genetic Drug Engineering, The University of Texas Southwestern Medical Center, Dallas, TX, U.S.A.

[2]Department of Hematology, St. Jude Children's Research Hospital, Memphis, TN, U.S.A.

[3]Department of Physiology, University of Texas Southwestern Medical Center, Dallas, TX, U.S.A.

[4]Merkin Institute of Transformative Technologies in Healthcare, Broad Institute of Harvard and MIT, Cambridge, MA, U.S.A.

[5]Department of Chemistry and Chemical Biology, Harvard University, Cambridge, MA, U.S.A.

[6]Howard Hughes Medical Institute, Harvard University, Cambridge, MA, U.S.A.

[7]Department of Genetic Medicine, Johns Hopkins University, Baltimore, MD, U.S.A.

*E-mail: Daniel.Siegwart@UTSouthwestern.edu

Table of Contents

Supplementary Materials and Methods

Materials

5A2-SC8 was synthesized and purified according to published protocols. Cholesterol, D-(+)-glucose, D-(+)-galactose, D-(+)-mannose, L-(-)-fucose, xylose, D-glucoronic acid, N-acetyl-D-glucosamine, N-acetyl-D-galactosamine, N-acetyl-D-mannosamine, Folic acid, Retinol, Biotin, Ascorbic acid, Ergocalciferol, (±)-α-Tocopherol, Dopamine hydrochloride, (−)-Norepinephrine, Acetylcholine chloride, Lauryl methacrylate, stearic acid N-succinimic ester, 5-Octylthieno[3,4-c]pyrrole-4,6-dione, Dodecyl isocyanate, Octyl isothiocyanate, (4,4,4-Trifluorobutyl)hydrazine hydrochloride, Trimellitic anhydride, Palmitic anhydride, Dodecyl aldehyde, (2,5-Dimethylphenethyl)hydrazine hydrochloride, CMC (N-Cyclohexyl-N′-(2-morpholinoethyl)carbodiimide methyl-p-toluenesulfonate), N,N'-Diisopropylcarbodiimide, EDC (1-Ethyl-3-(3-dimethylaminopropyl)carbodiimide), DCC (N,N'-Dicyclohexylcarbodiimide), 1-(3-Isothiocyanatobenzyl)-4-[2-(3,4-dihydro-2H-1-benzopyran-6-yl)-5-oxazolyl]pyridinium bromide, 3-Mercaptopropanyl-N-hydroxysuccinimide ester, DHSO (3,3′-Sulfinyldi(propanehydrazide)), SMPT (4-succinimidyloxycarbonyl-alpha-methyl-alpha(2-pyridyldithio)toluene), PDPH (3-(2-pyridyldithio)propionyl hydrazide), DFDNB (1,5-Difluoro-2,4-dinitrobenzene), Glutaraldehyde dioxime, Succinimidyl 4-formylbenzoate, Terephthaldehyde were purchased from Sigma Aldrich. N-acetylneuraminic acid, Arachidonic Acid, Docosahexaenoic Acid, Melatonin, Hydrocortisone, Estradiol, Tryptamine, 3-Iodothyronamine (hydrochloride), MEGA-10, n-Dodecyl-β-D-maltoside, α-C16 Galactosylceramide (d18:1/16:0), Sulfatides (bovine) (sodium salt), N-Oleoyl-L-Serine, N-(α-Linolenoyl) Tyrosine, N-Palmitoyl-L-Aspartate, N-Palmitoyl Glycine, N-Oleoyl Alanine, N-Oleoyl Glutamine, N-Oleoyl-L-phenylalanine, Acridinium NHS ester, DMABA NHS ester, Sulfosuccinimidyl Myristate (sodium salt), FMOC-Succinimide, 5-Norbornene-2-acetic acid succinimidyl ester, DSS (Disuccinimidyl Suberate), SMCC (Succinimidyl-4-(N-maleimidomethyl)cyclohexane-1-carboxylate) were purchased from Cayman Chemical. DOPE, 18:1 CDP DG (1,2-dioleoyl-sn-glycero-3-(cytidine diphosphate) (ammonium salt)), 18:1 PDP PE (1,2-dioleoyl-sn-glycero-3-phosphoethanolamine-N-[3-(2-pyridyldithio)propionate] (sodium salt)), 18:1 PE MCC (1,2-dioleoyl-sn-glycero-3-phosphoethanolamine-N-[4-(p-maleimidomethyl)cyclohexane-carboxamide] (sodium salt)), TMG-A13 (Tandem malonate glucoside-A13), VEG-3 (Vitamin-based Glycoside-3) were purchased from Avanti Polar Lipids. Hexadecylsuccinic Anhydride, 4-Methylbenzohydrazide, and Benzenesulfonyl Hydrazide were purchased from TCI. N-Dodecylacrylamide, Palmitic acid hydrazide were purchased from Fisher Scientific. TSAT (tris-(succinimidyl)aminotriacetate), and SIAB (succinimidyl (4-iodoacetyl)aminobenzoate) were purchased from Thermo Fisher. SIA (Succinimidyl iodoacetate), BS3 (bis(sulfosuccinimidyl)suberate), DSG (Di(N-succinimidyl) glutarate), DSP (dithiobis(succinimidyl propionate)), DSSeb (Disuccinimidyl sebacate), EGS (Ethylene glycolbis(succinimidylsuccinate)), SPDP (N-Succinimidyl 3-[2-pyridyldithio]-propionate), LC-SPDP (Succinimidyl 6-(3-[2-pyridyldithio]-propionamido)hexanoate) were purchased from Proteochem. 1-[3-(Dimethylamino)propyl]-3-ethylcarbodiimide methiodide was purchased from Santa Cruz Biotechnology. DMG-PEG 2000 was purchased from NOF America Corporation. Pur-A-Lyzer Midi Dialysis Kits (WMCO, 3.5 kDa) were purchased from Sigma Aldrich. D-Luciferin was purchased from Gold Biotechnology. 4',6-diamidino-2-phenylindole dihydrochloride (DAPI) was purchased from Thermo Fisher. Sucrose was purchased from Sigma Aldrich.The ReadyPrep 2-D Cleanup Kit, 12% Mini-PROTEAN TGX Precast Protein Gels, 2× Laemmli Buffer, and 10× Tris/Glycine/SDS were purchased from Bio-Rad. Innovative Research

C57BL/6 Mouse Plasma K2EDTA was purchased from Fisher Scientific. Firefly luciferase (Luc), Cre recombinase (Cre), Cas9 and ABE8e_NRCH mRNA were synthesized by in vitro transcription (IVT). Modified sgG34 and sgHBB were purchased from BioSprings.

Whole body biodistribution

C57BL/6 mice weighing 18 to 20 g were IV injected with various BM homing LNPs containing Cy5 Cre mRNA at a dose of 0.5 mg/kg mRNA. Ex vivo imaging (Cy5 channel) was performed 2 h post injection. Average fluorescence of the liver, spleen, lung, heart, kidney, and dissected bone were measured using Living Image Software (PerkinElmer) by drawing regions of interest around each organ.

***In vitro* murine erythrocyte differentiation**

Isolated Townes mice CD117+ cells were incubated in Erythroid Differentiation Medium, which is composed of IMDM (Sigma-Aldrich, I-3390) with 10 U/mL mouse erythropoietin (BioLegend, 587602), 10 ng/mL mSCF (BioLegend, 579708), 10 μM dexamethasone (Thermo Fisher, A17590.03), 15% FBS, 1% detoxified BSA (Sigma Aldrich, A7979), 200 μg/mL human holotransferrin (Sigma Aldrich, T0665), 10 μg/mL human insulin (Thermo Fisher, 12585014), 2 mM L-glutamine (Thermo Fisher, A2916801), 100 μM 2-mercaptoethanol (Thermo Fisher, 31350010), 1x penicillin-streptomycin, 100 ng/mL mIGF-1 (BioLegend, 591402) with a cell density of $2x10^5$ cells/mL alone or with 10 pg/cell C6-mDLNP containing ABE8e_NRCH mRNA and sgHBB (2/1 wt/wt) for 14 days. Genomic DNA was extracted from cells for Sanger sequencing to determine editing level. Ter119+ cells were isolated by magnetic separation, re-dispersed in 100 μL Erythroid Differentiation Medium in a 96 well plate and incubated under 1% O_2 for 18 hours. Cells were fixed with 2% glutaraldehyde (Sigma Aldrich, G6257) solution for 1 hour and subjected to imaging.

***In vivo* toxicity study**

C57BL/6J mice were IV injected with C6-LNPs at a Luc mRNA dose of 0.6 mg/kg. 24 hours and 7 days after injection, mice were anaesthetized with isoflurane, and blood samples were collected to obtain serum. Serum G-CSF, M-CSF, thrombopoietin, flt3, BALP, C3, C4a, and C5a levels were evaluated by enzyme-linked immunosorbent assay (ELISA) following standard protocol, and serum Ca and Phosphate levels were measured by VITROS MicroSlide™ technology.

Coding sequences for Luc, Cre, Cas9 and ABE8e_NRCH mRNAs

Firefly luciferase

ATGGAAGACGCCAAAAACATAAAGAAAGGCCCGGCGCCATTCTATCCGCTGGAAGATGGAACCG
CTGGAGAGCAACTGCATAAGGCTATGAAGAGATACGCCCTGGTTCCTGGAACAATTGCTTTTACA
GATGCACATATCGAGGTGGACATCACTTACGCTGAGTACTTCGAAATGTCCGTTCGGTTGGCAG
AAGCTATGAAACGATATGGGCTGAATACAAATCACAGAATCGTCGTATGCAGTGAAAACTCTCTT
CAATTCTTTATGCCGGTGTTGGGCGCGTTATTTATCGGAGTTGCAGTTGCGCCCGCGAACGACA
TTTATAATGAACGTGAATTGCTCAACAGTATGGGCATTTCGCAGCCTACCGTGGTGTTCGTTTCC
AAAAAGGGGTTGCAAAAAATTTTGAACGTGCAAAAAAAGCTCCCAATCATCCAAAAAATTATTATC
ATGGATTCTAAAACGGATTACCAGGGATTTCAGTCGATGTACACGTTCGTCACATCTCATCTACCT
CCCGGTTTTAATGAATACGATTTTGTGCCAGAGTCCTTCGATAGGGACAAGACAATTGCACTGAT

CATGAACTCCTCTGGATCTACTGGTCTGCCTAAAGGTGTCGCTCTGCCTCATAGAACTGCCTGCG
TGAGATTCTCGCATGCCAGAGATCCTATTTTTGGCAATCAAATCATTCCGGATACTGCGATTTTAA
GTGTTGTTCCATTCCATCACGGTTTTGGAATGTTTACTACACTCGGATATTTGATATGTGGATTTC
GAGTCGTCTTAATGTATAGATTTGAAGAAGAGCTGTTTCTGAGGAGCCTTCAGGATTACAAGATT
CAAAGTGCGCTGCTGGTGCCAACCCTATTCTCCTTCTTCGCCAAAAGCACTCTGATTGACAAATA
CGATTTATCTAATTTACACGAAATTGCTTCTGGTGGCGCTCCCCTCTCTAAGGAAGTCGGGGAAG
CGGTTGCCAAGAGGTTCCATCTGCCAGGTATCAGGCAAGGATATGGGCTCACTGAGACTACATC
AGCTATTCTGATTACACCCGAGGGGGATGATAAACCGGGCGCGGTCGGTAAAGTTGTTCCATTT
TTTGAAGCGAAGGTTGTGGATCTGGATACCGGGAAAACGCTGGGCGTTAATCAAAGAGGCGAAC
TGTGTGTGAGAGGTCCTATGATTATGTCCGGTTATGTAAACAATCCGGAAGCGACCAACGCCTTG
ATTGACAAGGATGGATGGCTACATTCTGGAGACATAGCTTACTGGGACGAAGACGAACACTTCTT
CATCGTTGACCGCCTGAAGTCTCTGATTAAGTACAAAGGCTATCAGGTGGCTCCCGCTGAATTG
GAATCCATCTTGCTCCAACACCCCAACATCTTCGACGCAGGTGTCGCAGGTCTTCCCGACGATG
ACGCCGGTGAACTTCCCGCCGCCGTTGTTGTTTTGGAGCACGGAAAGACGATGACGGAAAAAGA
GATCGTGGATTACGTCGCCAGTCAAGTAACAACCGCGAAAAAGTTGCGCGGAGGAGTTGTGTTT
GTGGACGAAGTACCGAAAGGTCTTACCGGAAAACTCGACGCAAGAAAAATCAGAGAGATCCTCA
TAAAGGCCAAGAAGGGCGGAAAGATCGCCGTGTAA

NLS-Cre

ATGCCCAAGAAGAAGAGGAAGGTGGCCAATTTACTGACCGTACACCAAAATTTGCCTGCATTACC
GGTCGATGCAACGAGTGATGAGGTTCGCAAGAACCTGATGGACATGTTCAGGGATCGCCAGGC
GTTTTCTGAGCATACCTGGAAAATGCTTCTGTCCGTTTGCCGGTCGTGGGCGGCATGGTGCAAG
TTGAATAACCGGAAATGGTTTCCCGCAGAACCTGAAGATGTTCGCGATTATCTTCTATATCTTCAG
GCGCGCGGTCTGGCAGTAAAAACTATCCAGCAACATTTGGGCCAGCTAAACATGCTTCATCGTC
GGTCCGGGCTGCCACGACCAAGTGACAGCAATGCTGTTTCACTGGTTATGCGGCGTATCCGAAA
AGAAAACGTTGATGCCGGTGAACGTGCAAAACAGGCTCTAGCGTTCGAACGCACTGATTTCGAC
CAGGTTCGTTCACTCATGGAAAATAGCGATCGCTGCCAGGATATACGTAATCTGGCATTTCTGGG
GATTGCTTATAACACCCTGTTACGTATAGCCGAAATTGCCAGGATCAGGGTTAAAGATATCTCAC
GTACTGACGGTGGGAGAATGTTAATCCATATTGGCAGAACGAAAACGCTGGTTAGCACCGCAGG
TGTAGAGAAGGCACTTAGCCTGGGGGTAACTAAACTGGTCGAGCGATGGATTTCCGTCTCTGGT
GTAGCTGATGATCCGAATAACTACCTGTTTTGCCGGGTCAGAAAAAATGGTGTTGCCGCGCCATC
TGCCACCAGCCAGCTATCAACTCGCGCCCTGGAAGGGATTTTTGAAGCAACTCATCGATTGATTT
ACGGCGCTAAGGATGACTCTGGTCAGAGATACCTGGCCTGGTCTGGACACAGTGCCCGTGTCG
GAGCCGCGCGAGATATGGCCCGCGCTGGAGTTTCAATACCGGAGATCATGCAAGCTGGTGGCT
GGACCAATGTAAATATTGTCATGAACTATATCCGTAACCTGGATAGTGAAACAGGGGCAATGGTG
CGCCTGCTGGAAGATGGCGATTAA

NLS-Cas9-SV40 NLS-Nucleoplasmin NLS

ATGCGCGCCGCTCCGGCAGCTAAGAAAAAGAAACTGGATGGCAGCGTCGACATGGATAAGAAAT
ACTCAATAGGCTTAGATATCGGCACAAATAGCGTCGGATGGGCGGTGATCACTGATGAATATAAG
GTTCCGTCTAAAAAGTTCAAGGTTCTGGGAAATACAGACCGCCACAGTATCAAAAAAAATCTTATA
GGGGCTCTTTTATTTGACAGTGGAGAGACAGCGGAAGCGACTCGTCTCAAACGGACAGCTCGTA
GAAGGTATACACGTCGGAAGAATCGTATTTGTTATCTACAGGAGATTTTTTCAAATGAGATGGCG

AAAGTAGATGATAGTTTCTTTCATCGACTTGAAGAGTCTTTTTTGGTGGAAGAAGACAAGAAGCAT
GAACGTCATCCTATTTTTGGAAATATAGTAGATGAAGTTGCTTATCATGAGAAATATCCAACTATC
TATCATCTGCGAAAAAAATTGGTAGATTCTACTGATAAAGCGGATTTGCGCTTAATCTATTTGGCC
TTAGCGCATATGATTAAGTTTCGTGGTCATTTTTTGATTGAGGGAGATTTAAATCCTGATAATAGT
GATGTGGACAAACTATTTATCCAGTTGGTACAAACCTACAATCAATTATTTGAAGAAAACCCTATT
AACGCAAGTGGAGTAGATGCTAAAGCGATTCTTTCTGCACGATTGAGTAAATCAAGACGATTAGA
AAATCTCATTGCTCAGCTCCCCGGTGAGAAGAAAAATGGCTTATTTGGGAATCTCATTGCTTTGT
CATTGGGTTTGACCCCTAATTTTAAATCAAATTTTGATTTGGCAGAAGATGCTAAATTACAGCTTTC
AAAAGATACTTACGATGATGATTTAGATAATTTATTGGCGCAAATTGGAGATCAATATGCTGATTT
GTTTTTGGCAGCTAAGAATTTATCAGATGCTATTTTACTTTCAGATATCCTAAGAGTAAATACTGAA
ATAACTAAGGCTCCCCTATCAGCTTCAATGATTAAACGCTACGATGAACATCATCAAGACTTGACT
CTTTTAAAAGCTTTAGTTCGACAACAACTTCCAGAAAAGTATAAAGAAATCTTTTTTGATCAATCAA
AAAACGGATATGCAGGTTATATTGATGGGGGAGCTAGCCAAGAAGAATTTTATAAATTTATCAAAC
CAATTTTAGAAAAAATGGATGGTACTGAGGAATTATTGGTGAAACTAAATCGTGAAGATTTGCTGC
GCAAGCAACGGACCTTTGACAACGGCTCTATTCCCCATCAAATTCACTTGGGTGAGCTGCATGCT
ATTTTGAGAAGACAAGAAGACTTTTATCCATTTTTAAAAGACAATCGTGAGAAGATTGAAAAAATC
TTGACTTTTCGAATTCCTTATTATGTTGGTCCATTGGCGCGTGGCAATAGTCGTTTTGCATGGATG
ACTCGGAAGTCTGAAGAAACAATTACCCCATGGAATTTTGAAGAAGTTGTCGATAAAGGTGCTTC
AGCTCAATCATTTATTGAACGCATGACAAACTTTGATAAAAATCTTCCAAATGAAAAAGTACTACC
AAAACATAGTTTGCTTTATGAGTATTTTACGGTTTATAACGAATTGACAAAGGTCAAATATGTTACT
GAAGGAATGCGAAAACCAGCATTTCTTTCAGGTGAACAGAAGAAAGCCATTGTTGATTTACTCTT
CAAAACAAATCGAAAAGTAACCGTTAAGCAATTAAAAGAAGATTATTTCAAAAAAATAGAATGTTTT
GATAGTGTTGAAATTTCAGGAGTTGAAGATAGATTTAATGCTTCATTAGGTACCTACCATGATTTG
CTAAAAATTATTAAAGATAAAGATTTTTTGGATAATGAAGAAAATGAAGATATCTTAGAGGATATTG
TTTTAACATTGACCTTATTTGAAGATAGGGAGATGATTGAGGAAAGACTTAAAACATATGCTCACC
TCTTTGATGATAAGGTGATGAAACAGCTTAAACGTCGCCGTTATACTGGTTGGGGACGTTTGTCT
CGAAAATTGATTAATGGTATTAGGGATAAGCAATCTGGCAAAACAATATTAGATTTTTTGAAATCA
GATGGTTTTGCCAATCGCAATTTTATGCAGCTGATCCATGATGATAGTTTGACATTTAAAGAAGAC
ATTCAAAAAGCACAAGTGTCTGGACAAGGCGATAGTTTACATGAACATATTGCAAATTTAGCTGGT
AGCCCTGCTATTAAAAAAGGTATTTTACAGACTGTAAAAGTTGTTGATGAATTGGTCAAAGTAATG
GGGCGGCATAAGCCAGAAAATATCGTTATTGAAATGGCACGTGAAAATCAGACAACTCAAAAGG
GCCAGAAAAATTCGCGAGAGCGTATGAAACGAATCGAAGAAGGTATCAAAGAATTAGGAAGTCA
GATTCTTAAAGAGCATCCTGTTGAAAATACTCAATTGCAAAATGAAAAGCTCTATCTCTATTATCTC
CAAAATGGAAGAGACATGTATGTGGACCAAGAATTAGATATTAATCGTTTAAGTGATTATGATGTC
GATCACATTGTTCCACAAAGTTTCCTTAAAGACGATTCAATAGACAATAAGGTCTTAACGCGTTCT
GATAAAAATCGTGGTAAATCGGATAACGTTCCAAGTGAAGAAGTAGTCAAAAAGATGAAAAACTA
TTGGAGACAACTTCTAAACGCCAAGTTAATCACTCAACGTAAGTTTGATAATTTAACGAAAGCTGA
ACGTGGAGGTTTGAGTGAACTTGATAAAGCTGGTTTTATCAAACGCCAATTGGTTGAAACTCGCC
AAATCACTAAGCATGTGGCACAAATTTTGGATAGTCGCATGAATACTAAATACGATGAAAATGATA
AACTTATTCGAGAGGTTAAAGTGATTACCTTAAAATCTAAATTAGTTTCTGACTTCCGAAAAGATTT
CCAATTCTATAAAGTACGTGAGATTAACAATTACCATCATGCCCATGATGCGTATCTAAATGCCGT
CGTTGGAACTGCTTTGATTAAGAAATATCCAAAACTTGAATCGGAGTTTGTCTATGGTGATTATAA
AGTTTATGATGTTCGTAAAATGATTGCTAAGTCTGAGCAAGAAATAGGCAAAGCAACCGCAAAAT

ATTTCTTTTACTCTAATATCATGAACTTCTTCAAAACAGAAATTACACTTGCAAATGGAGAGATTCG
CAAACGCCCTCTAATCGAAACTAATGGGGAAACTGGAGAAATTGTCTGGGATAAAGGGCGAGAT
TTTGCCACAGTGCGCAAAGTATTGTCCATGCCCCAAGTCAATATTGTCAAGAAAACAGAAGTACA
GACAGGCGGATTCTCCAAGGAGTCAATTTTACCAAAAAGAAATTCGGACAAGCTTATTGCTCGTA
AAAAAGACTGGGATCCAAAAAAATATGGTGGTTTTGATAGTCCAACGGTAGCTTATTCAGTCCTA
GTGGTTGCTAAGGTGGAAAAAGGGAAATCGAAGAAGTTAAAATCCGTTAAAGAGTTACTAGGGAT
CACAATTATGGAAAGAAGTTCCTTTGAAAAAAATCCGATTGACTTTTTAGAAGCTAAAGGATATAA
GGAAGTTAAAAAAGACTTAATCATTAAACTACCTAAATATAGTCTTTTTGAGTTAGAAAACGGTCG
TAAACGGATGCTGGCTAGTGCCGGAGAATTACAAAAAGGAAATGAGCTGGCTCTGCCAAGCAAA
TATGTGAATTTTTTATATTTAGCTAGTCATTATGAAAAGTTGAAGGGTAGTCCAGAAGATAACGAA
CAAAAACAATTGTTTGTGGAGCAGCATAAGCATTATTTAGATGAGATTATTGAGCAAATCAGTGAA
TTTTCTAAGCGTGTTATTTTAGCAGATGCCAATTTAGATAAAGTTCTTAGTGCATATAACAAACATA
GAGACAAACCAATACGTGAACAAGCAGAAAATATTATTCATTTATTTACGTTGACGAATCTTGGAG
CTCCCGCTGCTTTTAAATATTTTGATACAACAATTGATCGTAAACGATATACGTCTACAAAAGAAG
TTTTAGATGCCACTCTTATCCATCAATCCATCACTGGTCTTTATGAAACACGCATTGATTTGAGTC
AGCTAGGAGGTGACACCGGTGGTGGTCCCGGGGGTGGTGCGGCCGCAGGCAGCGGAAGCCCT
AAGAAAAAACGAAAAGTTGGCAGCGGAAGCAAAAGGCCGGCGGCCACGAAAAAGGCCGGCCAG
GCAAAAAAGAAAAAGTGA

SV40 NLS-ABE8e_NRCH-SV40 NLS

ATGGCCCCAAAGAAGAAGCGGAAAGTCTCTGAGGTGGAGTTTTCCCACGAGTACTGGATGAGAC
ATGCCCTGACCCTGGCCAAGAGGGCACGGGATGAGAGGGAGGTGCCTGTGGGAGCCGTGCTG
GTGCTGAACAATAGAGTGATCGGCGAGGGCTGGAACAGAGCCATCGGCCTGCACGACCCAACA
GCCCATGCCGAAATTATGGCCCTGAGACAGGGCGGCCTGGTCATGCAGAACTACAGACTGATTG
ACGCCACCCTGTACGTGACATTCGAGCCTTGCGTGATGTGCGCCGGCGCCATGATCCACTCTAG
GATCGGCCGCGTGGTGTTTGGCGTGAGGAACTCAAAAAGAGGCGCCGCAGGCTCCCTGATGAA
CGTGCTGAACTACCCCGGCATGAATCACCGCGTCGAAATTACCGAGGGAATCCTGGCAGATGAA
TGTGCCGCCCTGCTGTGCGATTTCTATCGGATGCCTAGACAGGTGTTCAATGCTCAGAAGAAGG
CCCAGAGCTCCATCAACTCCGGAGGATCTAGCGGAGGCTCCTCTGGCTCTGAGACACCTGGCA
CAAGCGAGAGCGCAACACCTGAAAGCAGCGGGGGCAGCAGCGGGGGGTCAGACAAGAAGTAC
AGCATCGGCCTGACCATCGGCACCAACTCTGTGGGCTGGGCCGTGATCACCGACGAGTACAAG
GTGCCCAGCAAGAAATTCAAGGTGCTGGGCAACACCGACCGGCACAGCATCAAGAAGAACCTG
ATCGGAGCCCTGCTGTTCGACAGCGGCGAAACAGCCGAGGCCACCCGGCTGAAGAGAACCGCC
AGAAGAAGATACACCAGACGGAAGAACCGGATCTGCTATCTGCAAGAGATCTTCAGCAACGAGA
TGGCCAAGGTGGACGACAGCTTCTTCCACAGACTGGAAGAGTCCTTCCTGGTGGAAGAGGATAA
GAAGCACGAGCGGCACCCCATCTTCGGCAACATCGTGGACGAGGTGGCCTACCACGAGAAGTA
CCCCACCATCTACCACCTGAGAAAGAAACTGGTGGACAGCACCGACAAGGCCGACCTGCGGCT
GATCTATCTGGCCCTGGCCCACATGATCAAGTTCCGGGGCCACTTCCTGATCGAGGGCGACCTG
AACCCCGACAACAGCGACGTGGACAAGCTGTTCATCCAGCTGGTGCAGACCTACAACCAGCTGT
TCGAGGAAAACCCCATCAACGCCAGCGGCGTGGACGCCAAGGCCATCCTGTCTGCCAGACTGA
GCAAGAGCAGACGGCTGGAAAATCTGATCGCCCAGCTGCCCGGCGAGAAGAAGAATGGCCTGT
TCGGAAACCTGATTGCCCTGAGCCTGGGCCTGACCCCCAACTTCAAGAGCAACTTCGACCTGGC
CGAGGATGCCAAACTGCAGCTGAGCAAGGACACCTACGACGACGACCTGGACAACCTGCTGGC

CCAGATCGGCGACCAGTACGCCGACCTGTTTCTGGCCGCCAAGAACCTGTCCGACGCCATCCT
GCTGAGCGACATCCTGAGAGTGAACACCGAGATCACCAAGGCCCCCCTGAGCGCCTCTATGGT
GAAGAGATACGACGAGCACCACCAGGACCTGACCCTGCTGAAAGCTCTCGTGCGGCAGCAGCT
GCCTGAGAAGTACAAAGAGATTTTCTTCGACCAGAGCAAGAACGGCTACGCCGGCTACATTGAC
GGCGGAGCCAGCCAGGAAGAGTTCTACAAGTTCATCAAGCCCATCCTGGAAAAGATGGACGGC
ACCGAGGAACTGCTCGTGAAGCTGAACAGAGAGGACCTGCTGCGGAAGCAGCGGACCTTCGAC
AACGGCATTATCCCCCACCAGATCCACCTGGGAGAGCTGCACGCCATTCTGCGGCGGCAGGGC
GATTTTTACCCATTCCTGAAGGACAACCGGGAAAAGATCGAGAAGATCCTGACCTTCCGCATCCC
CTACTACGTGGGCCCTCTGGCCAGGGGAAACAGCAGATTCGCCTGGATGACCAGAAAGAGCGA
GGAAACCATCACCCCCTGGAACTTCGAGGAAGTGGTGGACAAGGGCGCTTCCGCCCAGAGCTT
CATCGAGCGGATGACCAACTTCGATAAGAACCTGCCCAACGAGAAGGTGCTGCCCAAGCACAGC
CTGCTGTACGAGTACTTCACCGTGTATAACGAGCTGACCAAAGTGAAATACGTGACCGAGGGAA
TGAGAAAGCCCGCCTTCCTGAGCGGCGAGCAGAAAAAGGCCATCGTGGACCTGCTGTTCAAGA
CCAACCGGAAAGTGACCGTGAAGCAGCTGAAAGAGGACTACTTCAAGAAAATCGAGTGCTTCGA
CTCCGTGGAAATCTCCGGCGTGGAAGATCGGTTCAACGCCTCCCTGGGCACATACCACGATCTG
CTGAAAATTATCAAGGACAAGGACTTCCTGGACAATGAGGAAAACGAGGACATTCTGGAAGATAT
CGTGCTGACCCTGACACTGTTTGAGGACAGAGAGATGATCGAGGAACGGCTGAAAACCTATGCC
CACCTGTTCGACGACAAAGTGATGAAGCAGCTGAAGCGGCTGAGATACACCGGCTGGGGCAGG
CTGAGCCGGAAGCTGATCAACGGCATCCGGGACAAGCAGTCCGGCAAGACAATCCTGGATTTC
CTGAAGTCCGACGGCTTCGCCAACAGAAACTTCATGCAGCTGATCCACGACGACAGCCTGACCT
TTAAAGAGGACATCCAGAAAGCCCAGGTGTCCGGCCAGGGCGATAGCCTGCACGAGCACATTG
CCAATCTGGCCGGCAGCCCCGCCATTAAGAAGGGCATCCTGCAGACAGTGAAGGTGGTGGACG
AGCTCGTGAAAGTGATGGGCGGCCACAAGCCCGAGAACATCGTGATCGAAATGGCCAGAGAGA
ACCAGACCACCCAGAAGGGACAGAAGAACAGCCGCGAGAGAATGAAGCGGATCGAAGAGGGCA
TCAAAGAGCTGGGCAGCCAGATCCTGAAAGAACACCCCGTGGAAAACACCCAGCTGCAGAACG
AGAAGCTGTACCTGTACTACCTGCAGAATGGGCGGGATATGTACGTGGACCAGGAACTGGACAT
CAACCGGCTGTCCGACTACGATGTGGACCATATCGTGCCTCAGAGCTTTCTGAAGGACGACTCC
ATCGACAACAAGGTGCTGACCAGAAGCGACAAGAACCGGGGCAAGAGCGACAACGTGCCCTCC
GAAGAGGTCGTGAAGAAGATGAAGAACTACTGGCGGCAGCTGCTGAACGCCAAGCTGATTACCC
AGAGAAAGTTCGACAATCTGACCAAGGCCGAGAGAGGCGGCCTGAGCGAACTGGATAAGGCCG
GCTTCATCAAGAGACAGCTGGTGGAAACCCGGCAGATCACAAAGCACGTGGCACAGATCCTGGA
CTCCCGGATGAACACTAAGTACGACGAGAATGACAAGCTGATCCGGGAAGTGAAAGTGATCACC
CTGAAGTCCAAGCTGGTGTCCGATTTCCGGAAGGATTTCCAGTTTTACAAAGTGCGCGAGATCAA
CAACTACCACCACGCCCACGACGCCTACCTGAACGCCGTCGTGGGAACCGCCCTGATCAAAAA
GTACCCTAAGCTGGAAAGCGAGTTCGTGTACGGCGACTACAAGGTGTACGACGTGCGGAAGAT
GATCGCCAAGAGCGAGCAGGAAATCGGCAAGGCTACCGCCAAGTACTTCTTCTACAGCAACATC
ATGAACTTTTTCAAGACCGAGATTACCCTGGCCAACGGCGAGATCCGGAAGCGGCCTCTGATCG
AGACAAACGGCGAAACCGGGGAGATCGTGTGGGATAAGGGCCGGGATTTTGCCACCGTGCGGA
AAGTGCTGAGCATGCCCCAAGTGAATATCGTGAAAAAGACCGAGGTGCAGACAGGCGGCTTCAG
CAAAGAGTCTATCCTGCCCAAGGGTAACAGCGATAAGCTGATCGCCAGAAAGAAGGACTGGGAC
CCTAAGAAGTACGGCGGCTTCAACAGCCCCACCGTGGCCTATTCTGTGCTGGTGGTGGCCAAAG
TGGAAAAGGGCAAGTCCAAGAAACTGAAGAGTGTGAAAGAGCTGCTGGGGATCACCATCATGGA
AAGAAGCAGCTTCGAGAAGAATCCCATCGACTTTCTGGAAGCCAAGGGCTACAAAGAAGTGAAA

AAGGACCTGATCATCAAGCTGCCTAAGTACTCCCTGTTCGAGCTGGAAAACGGCCGGAAGAGAA
TGCTGGCCTCTGCCGGCGTGCTGCAGAAGGGAAACGAACTGGCCCTGCCCTCCAAATATGTGA
ACTTCCTGTACCTGGCCAGCCACTATGAGAAGCTGAAGGGCTCCCCCGAGGATAATGAGCAGAA
ACAGCTGTTTGTGGAACAGCACAAGCACTACCTGGACGAGATCATCGAGCAGATCAGCGAGTTC
TCCAAGAGAGTGATCCTGGCCGACGCTAATCTGGACAAAGTGCTGTCCGCCTACAACAAGCACC
GGGATAAGCCCATCAGAGAGCAGGCCGAGAATATCATCCACCTGTTTACCCTGACCAATCTGGG
AGCCCCTGCCGCCTTCAAGTACTTTGACACCACCATCAACCGGAAGCAATACAACACGACCAAA
GAGGTGCTGGACGCCACCCTGATCCGTCAGAGCATCACCGGCCTGTACGAGACACGGATCGAC
CTGTCTCAGCTGGGAGGTGACTCTGGCGGCTCAAAAAGAACCGCCGACGGCAGCGAATTCGAG
CCCAAGAAGAAGAGGAAAGTCTAA

Supplementary Results and Discussion

NHS reactive moiety leads to BM delivery tropism

Reasoning that SA-NHS contains a labile NHS group which may undergo hydrolysis in aqueous solution, we incorporated stearic acid, the hydrolysis product of SA-NHS, into LNPs and examined the *in vivo* delivery fate (**Supplementary Fig. 2**). We found that it did not lead to luciferase mRNA delivery to BM, indicating that the reactive lipid itself and not a potential hydrolysis product caused the BM tropism. The incorporation of an unreactive molecule with similar head group to NHS ester into LNPs also did not yield BM delivery (**Supplementary Fig. 2**). These two negative control results confirmed that SA-NHS, the covalent lipid species, drove the BM delivery tropism.

Covalent lipids lead to BM delivery in other 4-lipid formulations

We examined if the BM homing capability of covalent lipid species can be preserved when incorporated in other established 4-component LNP systems. We selected ALC-0315 and SM-102 based LNPs, which have been administered to billions of people around the world as the COVID-19 vaccines developed by Pfizer/BioNTech and Moderna, respectively.[1] We incorporated 20 mol. % AA11 in SM-102 and ALC-0315 LNPs encapsulating Luc mRNA, IV injected into C57BL6 mice, and conducted *ex vivo* organ imaging 6 hours after LNP injection. The BM homing capability of AA11 was well maintained when incorporated in SM-102 or ALC-0315 based LNPs, demonstrating successful modularity of the approach. 5A2-SC8 led to higher efficacy versus SM-102 and ALC-0315 (**Supplementary Fig. 4**), and was used in further studies. Thus, we show that BM homing capability of covalent lipid species is generally applicable to other classes of ionizable cationic lipid LNPs, which could facilitate a clinical path to tackle hematopoietic diseases.

Molar percentage study of covalent lipid species in 5-lipid formulations

Previous studies showed that specific molar percentages of lipid components maximized LNP delivery efficacy in different tissues.[2] We thus studied if altering the molar percentage of covalent lipid species would change transfection efficacy in BM. We prepared Cre mRNA encapsulated LNPs with 10, 20, and 30 molar percentage of AA11, IV injected into tdTom mice, and analyzed $tdTom^+$ cells in different cell types. Increasing AA11 molar ratio from 10% to 20% did not change delivery efficacy to all analyzed cell types, while further increasing to 30% led to dramatic decrease in transfection efficacy across all cell types, especially in hematopoietic stem and progenitor cells, which are the most therapeutically relevant cell types in this study (**Supplementary Fig. 11**). Therefore, to maintain delivery efficacy and to effectively present covalent lipid species on LNP, we used 20 % covalent lipid species for the rest of the studies.

Storage stability study of BM homing LNP

To study if BM homing LNPs are prone to transfection activity loss due to lipid or mRNA degradation or LNP instability, we IV injected 20 mol% palmitic hydrazide (C6) LNP containing Cre mRNA that had been stored at room temperature, 4 ^oC, or -20 ^oC for 3 days into tdTom mice. tdTom+% in each cell type were analyzed using flow cytometry. Maintenance of LNP transfection activity after 3 days storage at 4 ^oC was clearly observed as there was no significant difference in tdTom+% in any analyzed cell types, while room temperature and -20 ^oC storage both led to significant decrease in transfection capability, including in hematopoietic stem and progenitor cells (**Supplementary Fig. 12**).

Hydrodynamic diameter and PDI studies of 20 mol% C6 LNPs under different storage conditions also mirrored the above results (**Supplementary Fig. 13**). These results indicated that freshly prepared and 4 ^{o}C stored LNPs could be used in further studies.

In vivo toxicity studies of BM homing LNP

To establish the *in vivo* safety profiles of covalent lipid containing LNPs, we have conducted the following studies. First, we measured the whole body biodistribution of BM homing LNP formulations encapsulating Cy5 labeled mRNA. Little abnormal accumulation was observed in liver, spleen, lung, heart, and kidney, while some formulations demonstrated enhanced accumulation in BM compared with LNP controls (**Supplementary Fig. 20**). We also measured the serum level of 10 bone and bone marrow related biomarkers after BM homing LNP administration. Some biomarkers demonstrated elevated or decreased serum levels 24 hours after LNP injection, which is in accordance to previous reports that serum level of certain cytokines increased shortly after LNP injection but resolved to basal level afterwards.[3, 4] More importantly, all measured biomarkers returned to basal level 7 days after LNP injection (**Supplementary Fig. 21-23**). This indicates that LNP associated perturbation in bone and bone marrow metabolism can be quickly relieved and may cause less side effects than previous studies using adeno-associated virus or nanoparticle delivery approaches.[5-7] Moreover, we detected Cas9 endonuclease and ABE8e_NRCH base editing in major organs of Townes mice receiving IV LNP administration, in which no editing was detected in reproductive organs (**Supplementary Fig. 24**). All the above results reduce *in vivo* toxicity concerns on the non-specific reactivity of covalent lipid species.

Discussion

The idea of incorporating reactive lipid species in LNPs was inspired by the success of covalent drugs, which were initially viewed as risky but turned out to be effective and possess advantages in specificity.[8] Covalent drugs have recently gained more attention as they have been involved in the drug design for next-generation drugs, such as in the evolution of targeted covalent inhibitors and covalent PROTACs.[8, 9] These advances suggest the safety tolerance of covalent bond forming molecules for both academic research and pharmaceutical industry. The results of *in vivo* toxicity studies of BM homing LNPs demonstrated the lack of nonspecific binding and toxicity relevant to the covalent lipid species. Moreover, the excellent maintenance of *in vivo* transfection efficacy of BM homing LNPs following storage and subsequent administration suggest that mRNA reactions and *in vivo* degradation of covalent lipid species are likely not occurring.[10]

Initial results suggest that bone marrow enrichment is closely related to ApoE in the serum, as evidenced by the significant decrease in delivery efficacy in ApoE$^{-/-}$ mice. The details of how covalent lipids and crosslinkers interact with serum proteins, especially ApoE, as well as how these interactions lead to bone marrow tropism other than liver delivery (liver delivering LNPs also heavily rely on ApoE to achieve liver tropism) still remain to be explored. It is possible that differences in the conformation of surface-bound ApoE exist between BM homing LNPs compared to LNP, which enable interactions with relevant ApoE receptors expressed by the bone marrow, leading to bone marrow tropism. Indeed, other work has shown that structure and conformation of corona proteins can affect which receptors nanoparticles interact with and their pathway of cellular uptake.[11-13]

Reference

1. Chaudhary, N., Weissman, D. & Whitehead, K.A. mRNA vaccines for infectious diseases: principles, delivery and clinical translation. *Nat. Rev. Drug Discov.* **20**, 817-838 (2021).
2. Cheng, Q. et al. Selective organ targeting (SORT) nanoparticles for tissue-specific mRNA delivery and CRISPR-Cas gene editing. *Nat. Nanotechnol.* **15**, 313-320 (2020).
3. Maugeri, M. et al. Linkage between endosomal escape of LNP-mRNA and loading into EVs for transport to other cells. *Nat. Commun.* **10**, 4333 (2019).
4. Ramaswamy, S. et al. Systemic delivery of factor IX messenger RNA for protein replacement therapy. *Proc. Natl. Acad. Sci. USA* **114**, E1941-E1950 (2017).
5. Christos, M.S. et al. Adeno-associated virus (AAV) reduces cortical dendritic complexity in a TLR9-dependent manner. *bioRxiv*, 2021.2009.2028.462148 (2021).
6. Emami, M.R. et al. Innate and adaptive AAV-mediated immune responses in a mouse model of Duchenne muscular dystrophy. *Mol. Ther. Methods Clin. Dev.* **30**, 90-102 (2023).
7. Luo, Z. et al. Neutrophil hitchhiking for drug delivery to the bone marrow. *Nat. Nanotechnol.* **18**, 647-656 (2023).
8. Singh, J., Petter, R.C., Baillie, T.A. & Whitty, A. The resurgence of covalent drugs. *Nat. Rev. Drug Discov.* **10**, 307-317 (2011).
9. Grimster, N.P. Covalent PROTACs: the best of both worlds? *RSC Med. Chem.* **12**, 1452-1458 (2021).
10. Packer, M., Gyawali, D., Yerabolu, R., Schariter, J. & White, P. A novel mechanism for the loss of mRNA activity in lipid nanoparticle delivery systems. *Nat. Commun.* **12**, 6777 (2021).
11. Fleischer, C.C. & Payne, C.K. Secondary structure of corona proteins determines the cell surface receptors used by nanoparticles. *J Phys Chem B* **118**, 14017-14026 (2014).
12. Myerson, J.W. et al. Supramolecular arrangement of protein in nanoparticle structures predicts nanoparticle tropism for neutrophils in acute lung inflammation. *Nat. Nanotechnol.* **17**, 86-97 (2022).
13. Zhang, Y., Wu, J.L.Y., Lazarovits, J. & Chan, W.C.W. An analysis of the binding function and structural organization of the protein corona. *J Am Chem Soc* **142**, 8827-8836 (2020).

Supplementary Figures

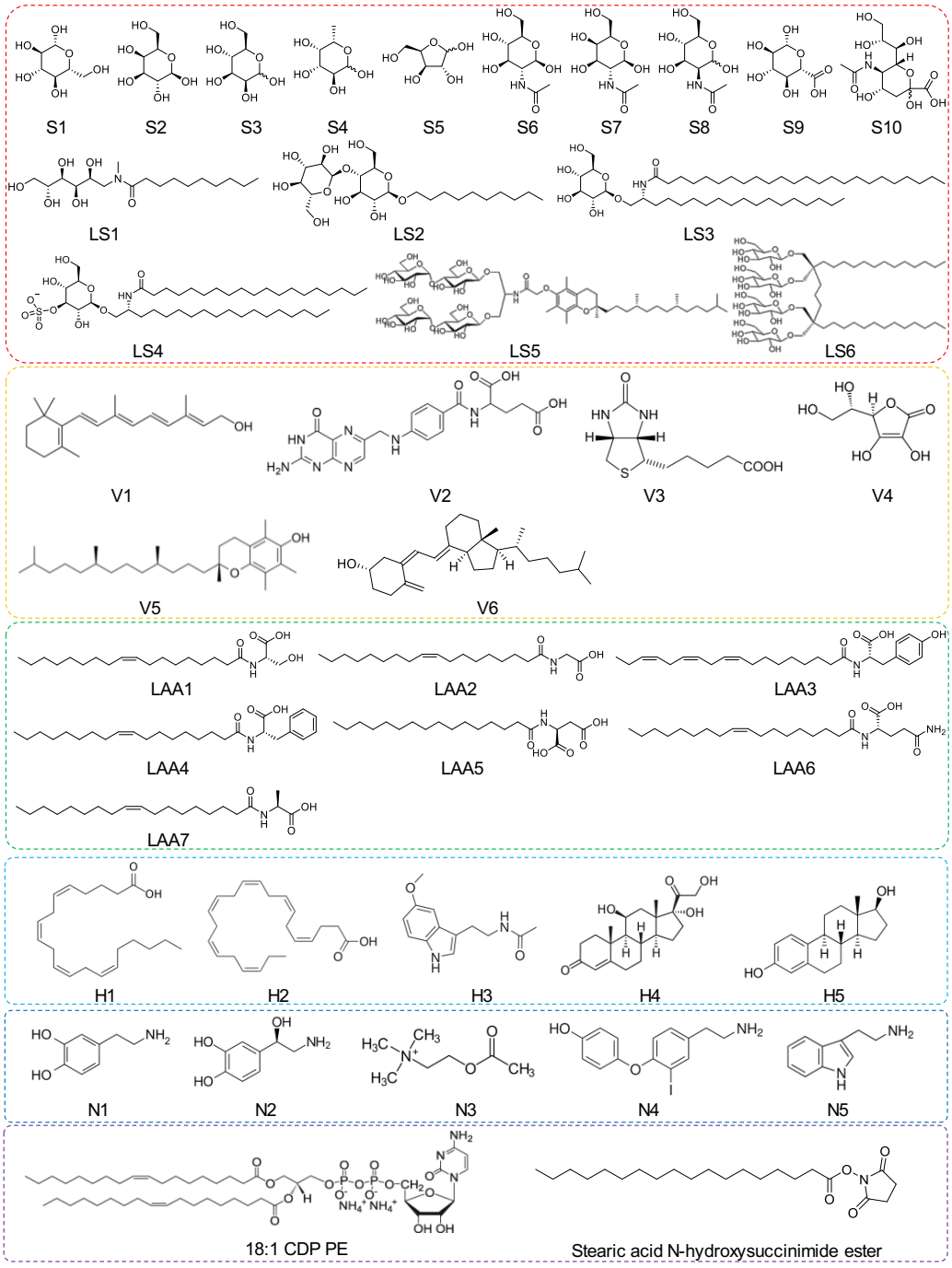

Supplementary Fig. 1 | Molecular structures of tested biologically active molecules as SORT lipids in search for novel in vivo mRNA delivery tropism. Red: 16 sugar and lipidized sugar molecules. Orange: 6 vitamin molecules. Green: 7 lipidized amino acid molecules. Cyan: 5 hormone molecules. Blue: 5 neurotransmitter molecules. Purple: 1 lipidized nucleotide and 1 N-hydroxysuccinimide ester lipid.

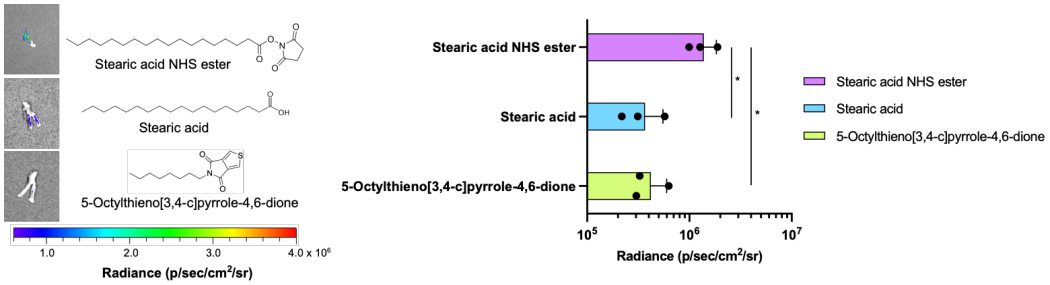

Supplementary Fig. 2 | Bioluminescence image of dissected femurs collected from mouse injected with 20% stearic acid NHS ester-LNP, 20% stearic acid-LNP, and 20% 5-Octylthieno[3,4-c]pyrrole-4,6-dione-LNP formulations, the molecular structures of tested molecules, and average luminescence intensity of dissected femurs. N=3, femurs were collected 6 hours after injection. Data are presented as mean ± s.d. (n = 3 biologically independent samples). *P < 0.05 determined by one-way ANOVA with multiple-comparison test.

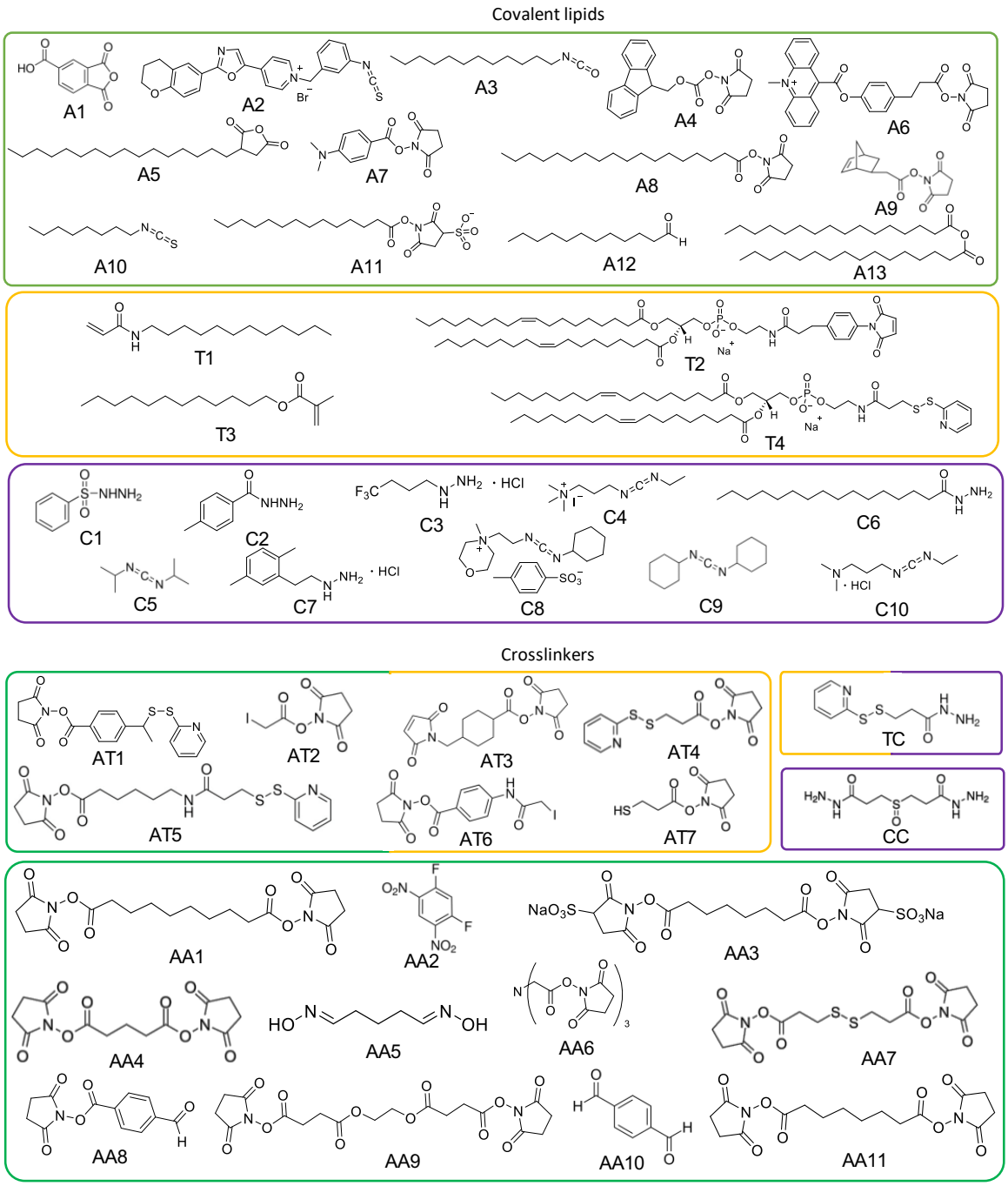

Supplementary Fig. 3 | Molecular structures of tested covalent lipids (green, orange and purple) and crosslinkers (green-orange, orange-purple, purple, and green). Covalent lipid: molecules in 1) green box are reactive to amines; 2) orange box are reactive to thiols; 3) purple box are reactive to carboxylic acids. Crosslinkers: molecules in 1) green-orange box are reactive to amines and thiols; 2) orange-purple box are reactive to thiols and carboxylic acids; 3) purple box are reactive to carboxylic acids; 4) green box are reactive to amines.

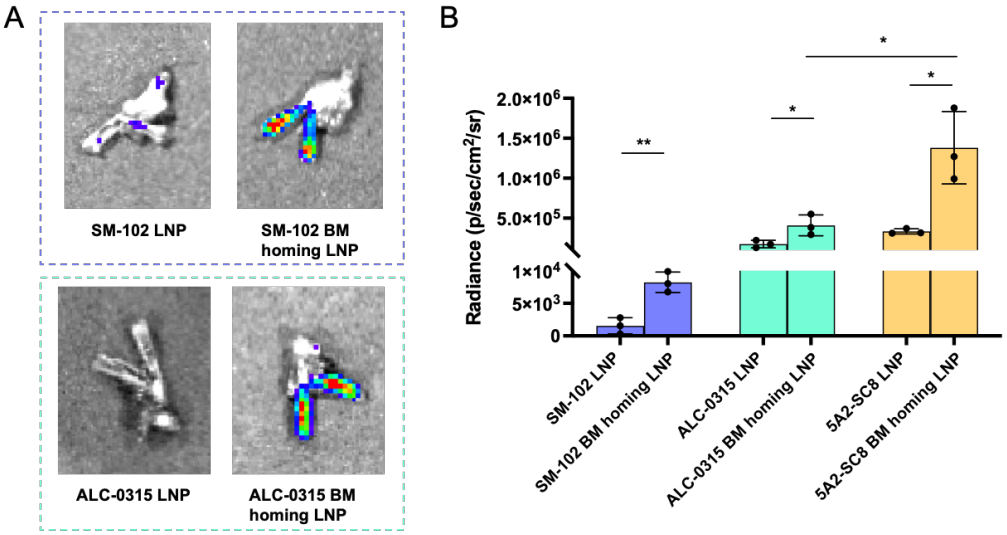

Supplementary Fig. 4 | Bone marrow transfection by SM-102, ALC-0315, and 5A2-SC8 based formulations. (**A**) Representative bioluminescence images and (**B**) average bioluminescence signal intensity of dissected femurs. Mice received IV injection of SM-102/ALC-0315/5A2-SC8 LNPs or AA11-LNPs and encapsulating Luc mRNA. Ex vivo imaging was conducted 6 hours after injection. Data are presented as mean ± s.d. (n = 3 biologically independent samples). *P < 0.05, **P < 0.01 determined by two-tailed t-test.

PBS hematopoietic stem and progenitor cell (HSPC) gating strategy

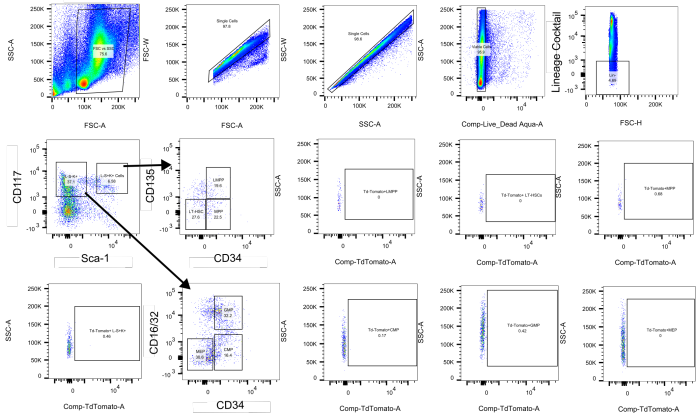

A11 hematopoietic stem and progenitor cell (HSPC) gating strategy

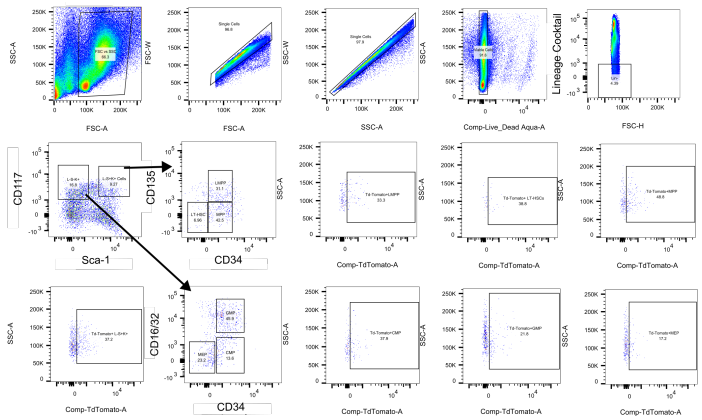

Supplementary Fig. 5 | The FACS gating strategy for analysis of tdTom+ cells in hematopoietic stem and progenitor cells (HSPCs) are presented. Live-Dead aqua was used to distinguish live cells. Lineage cocktail assay was used to distinguish Lin- cell populations. CD117 and Sca-1 were used to distinguish $L^-S^-K^+$ and $L^-S^+K^+$ populations. CD34 and CD135 were used to distinguish LT-HSC, LMPP and MPP in $L^-S^+K^+$ cells. CD34 and CD16/32 were used to distinguish MEP, CMP and GMP in $L^-S^-K^+$ cells.

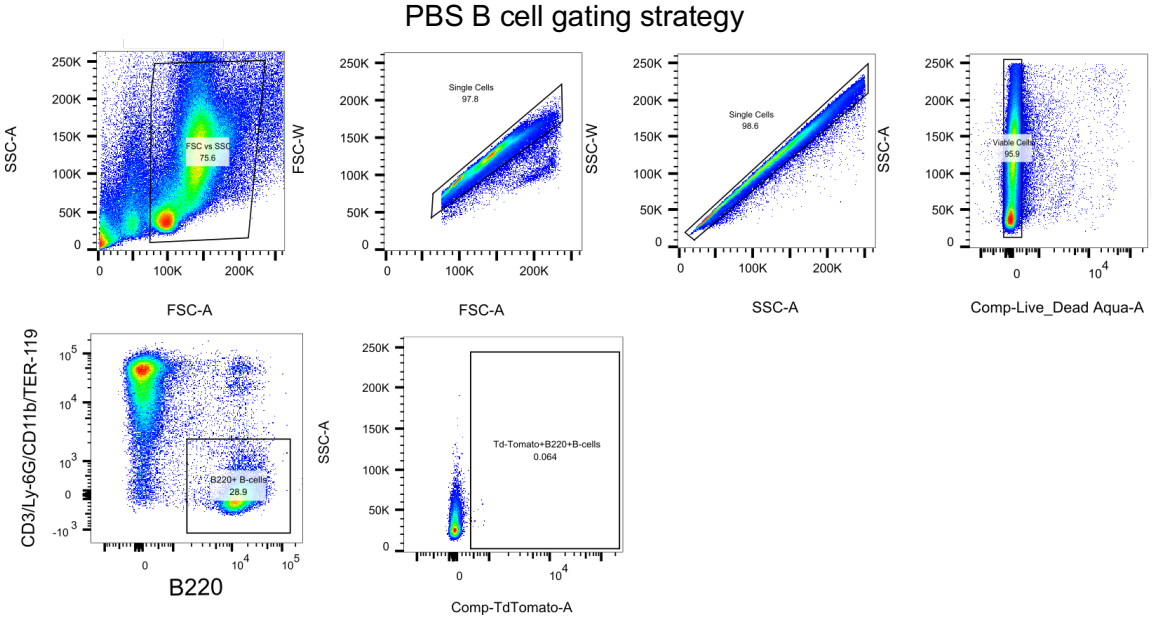

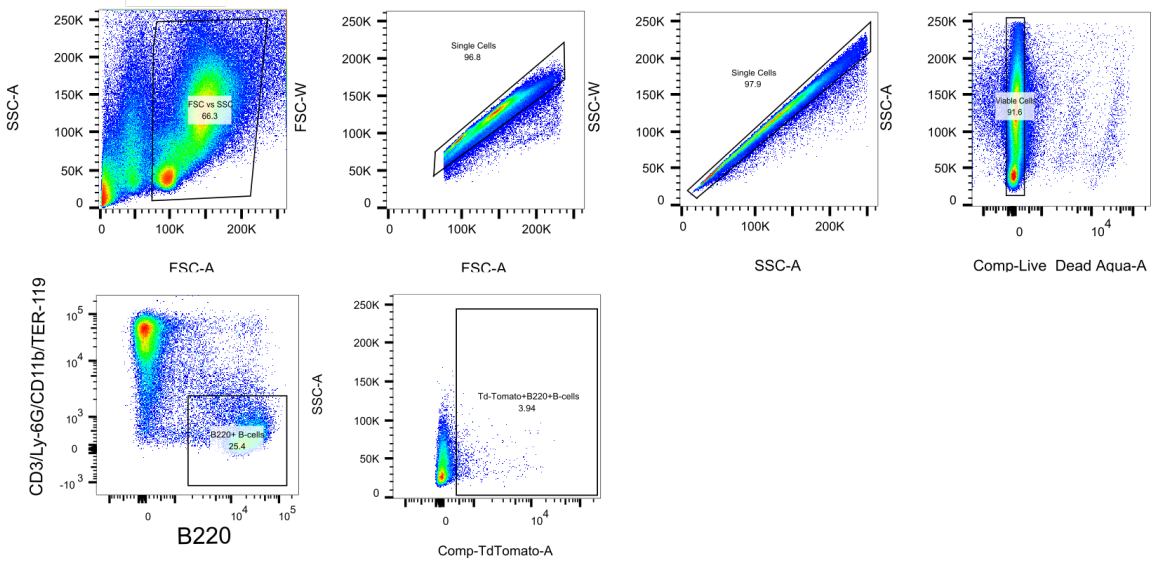

Supplementary Fig. 6 | The FACS gating strategy for analysis of tdTom+ cells in B cells are presented. Live-Dead aqua was used to distinguish live cells. B220 and CD3, Ly-6G, CD11b, and TER-119 were used to distinguish B cells.

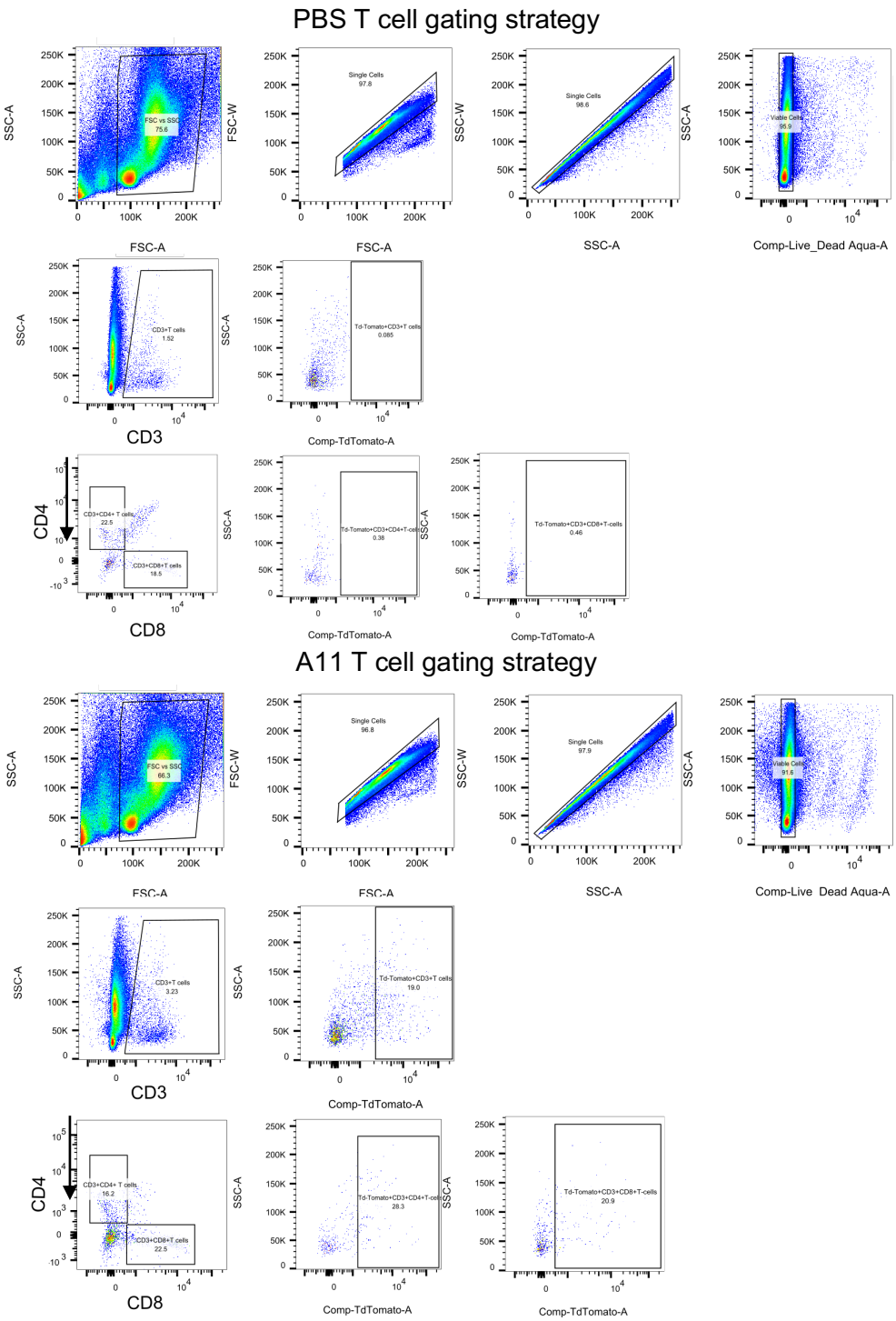

Supplementary Fig. 7 | The FACS gating strategy for analysis of tdTom+ cells in T cells are presented. Live-Dead aqua was used to distinguish live cells. CD3 was used to distinguish T cells. CD4 and CD8 were used to distinguish CD4+ and CD8+ T cells, respectively.

PBS macrophages, monocytes and neutrophils gating strategy

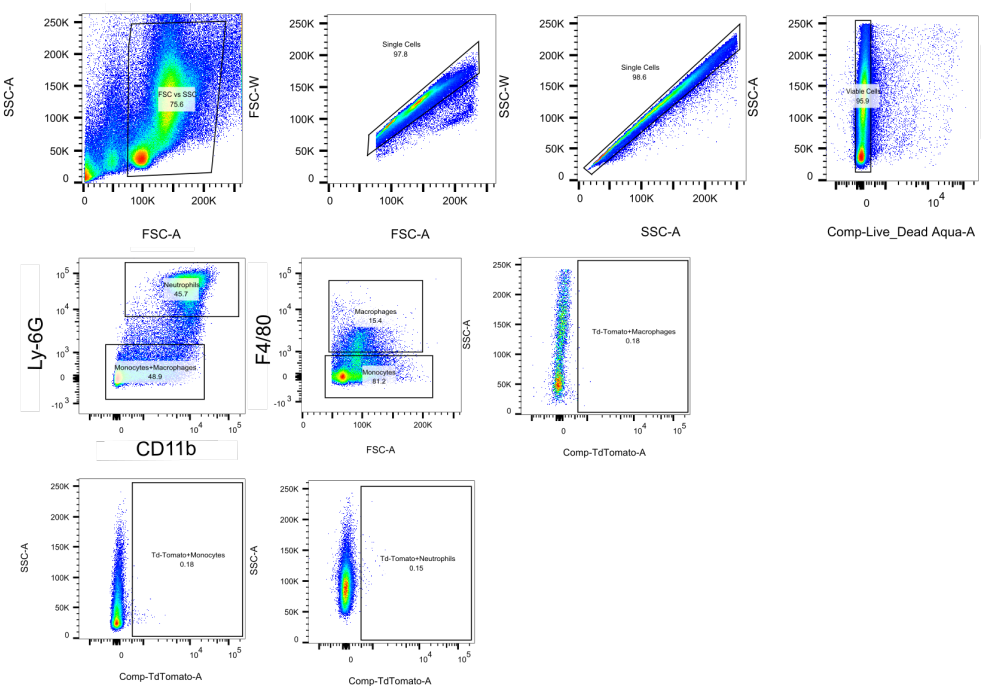

A11 macrophages, monocytes and neutrophils gating strategy

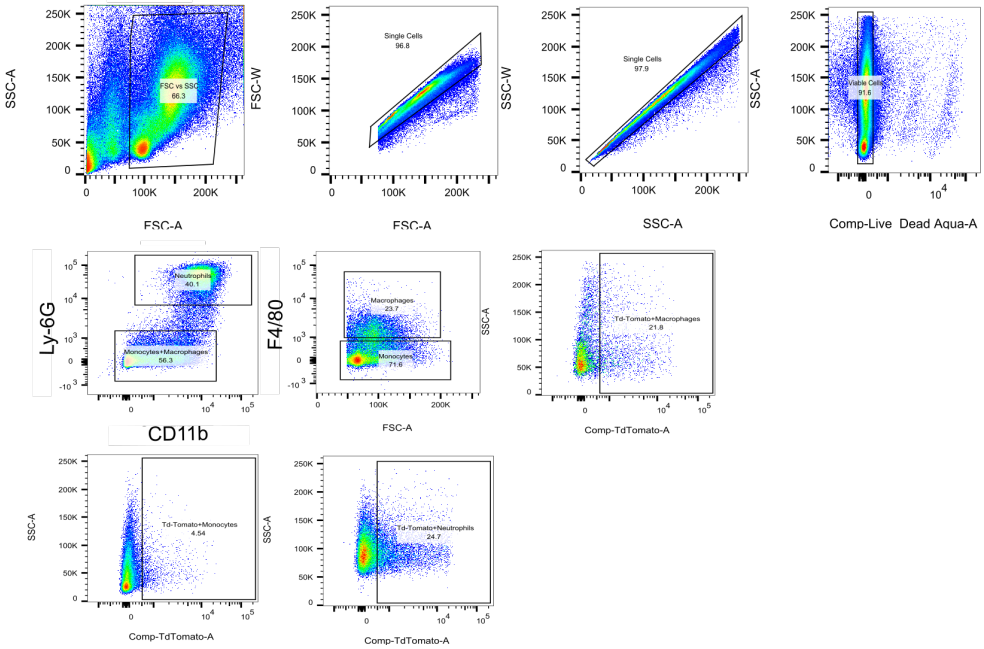

Supplementary Fig. 8 | The FACS gating strategy for analysis of tdTom+ cells in macrophage, monocytes and neutrophils are presented. Live-Dead aqua was used to distinguish live cells. CD11b and Ly-6G were used to distinguish neutrophils and macrophage/monocytes. F4/80 was used to distinguish macrophage and monocytes.

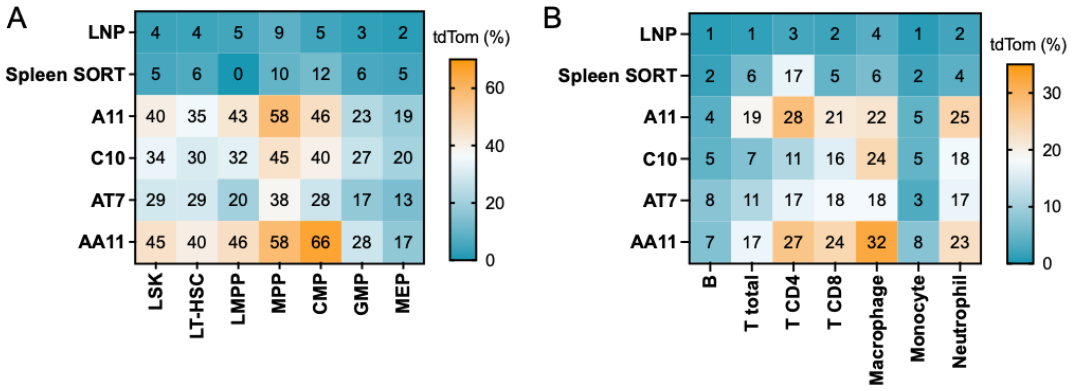

Supplementary Fig. 9 | Comparison of transfection in BM cells (stem and progenitor cells (**A**), mature immune cells (**B**)) by LNP and Spleen SORT spleen targeting (20% 18PA) formulation and lead BM homing formulations.

A

	LSK	LT-HSC	LMPP	MPP	CMP	GMP	MEP	B	T	T CD4	T CD8	Macrophage	Monocyte	Neutrophil
1 injection	36.9	32.2	22.7	56	50	22.9	10.3	6.72	8.15	15.7	13.9	23.4	6.59	12.9
2 injections	73.2	64.8	65.1	84.6	66.1	51.7	32	10	17.9	30.8	31.2	37.4	9.44	21.9

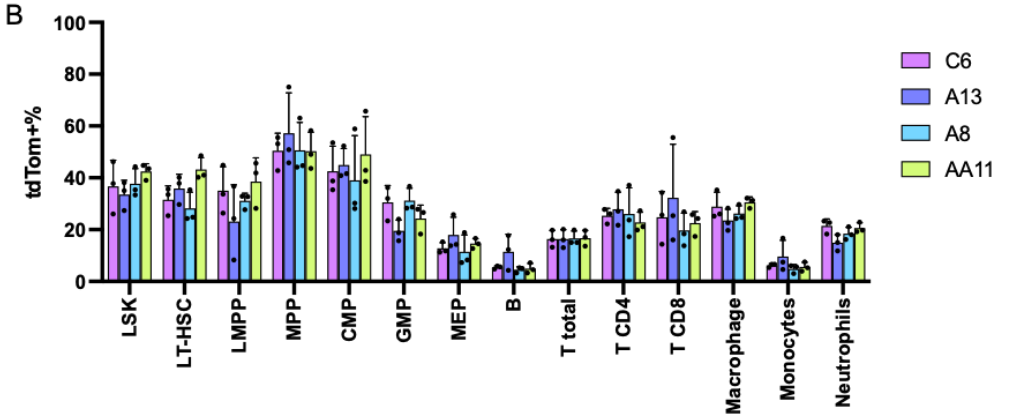

Supplementary Fig. 10 | (A) tdTom+% of each BM cell type after 1 or 2 AA11-LNP injections encapsulating Cre mRNA (0.6 mg/kg). Injection interval is 1 week for the 2 injections group and BM was harvested 3 days after the last injection. (B) n=3 for selected formulations delivering Cre mRNA into tdTomato mice. tdTom+% was determined by flow cytometry. Data are presented as mean ± s.d. (n = 3 biologically independent samples).

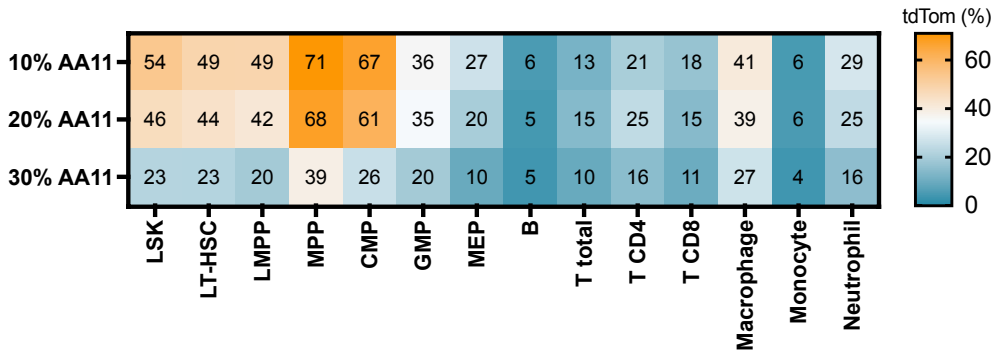

Supplementary Fig. 11 | tdTom+% of different bone marrow cell types isolated from tdTom mice receiving Cre mRNA encapsulated LNPs formulated with 10%, 20%, and 30% AA11. Samples were extracted 3 days after LNP injection and tdTom+% was determined by flow cytometry.

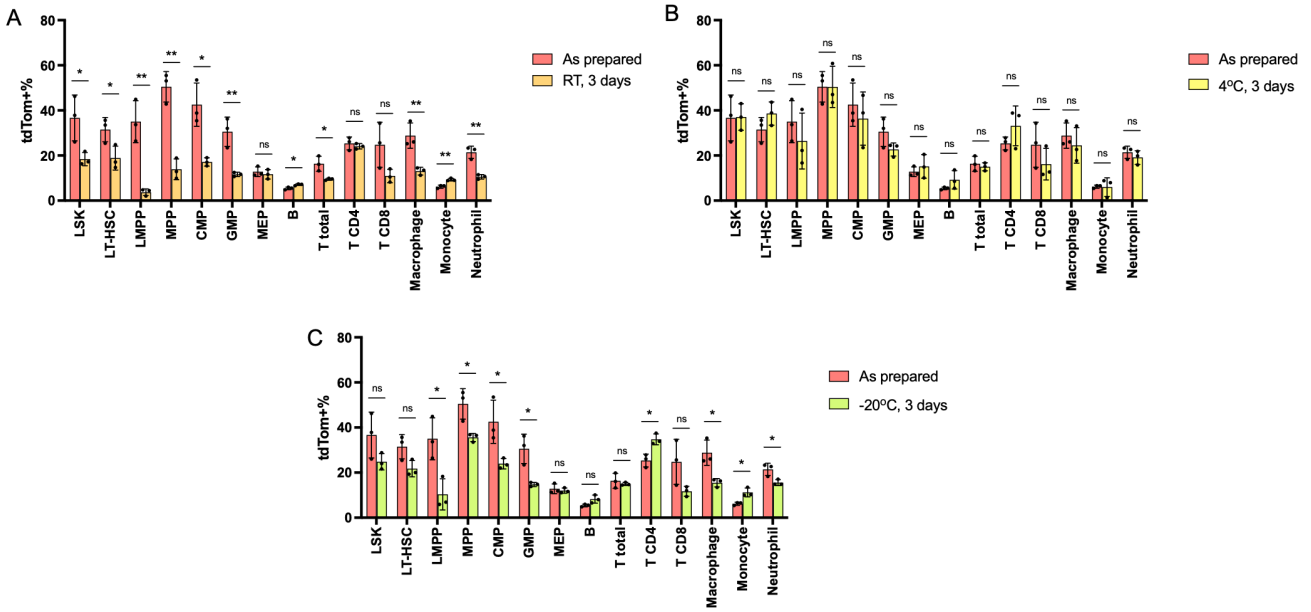

Supplementary Fig. 12 | tdTom+% in different bone marrow cell types isolated from animals receiving IV injection of bone marrow homing LNPs stored at different conditions. C6-mDLNP was injected in tdTom mice as prepared or stored at room temperature (**A**), 4 ºC (**B**) or -20 ºC (**C**) for 3 days. Bone marrow cells were extracted 3 days after LNP injection and tdTom+% was determined by flow cytometry. Data are presented as mean ± s.d. (n = 3 biologically independent samples). ns, no significant difference, **P* < 0.05, ***P* < 0.01 determined by two-tailed t-test.

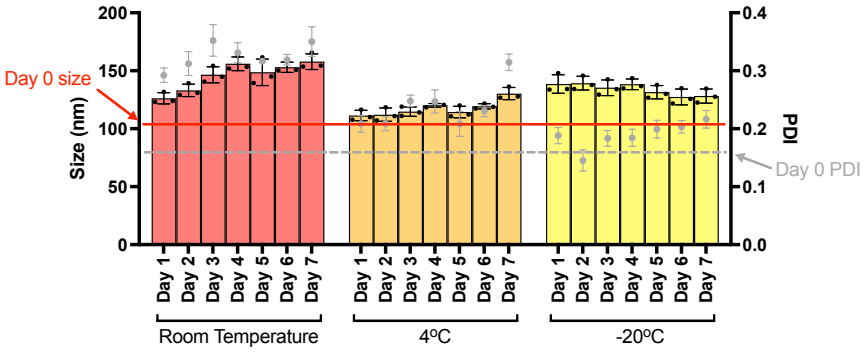

Supplementary Fig. 13 | Hydrodynamic diameter and PDI of C6-mDLNP stored at room temperature, 4° C, and -20 °C for up to 7 days. Red solid line and grey dotted line indicates hydrodynamic diameter and PDI of as-prepared LNPs, respectively. Data are presented as mean ± s.d. (n = 3 biologically independent samples).

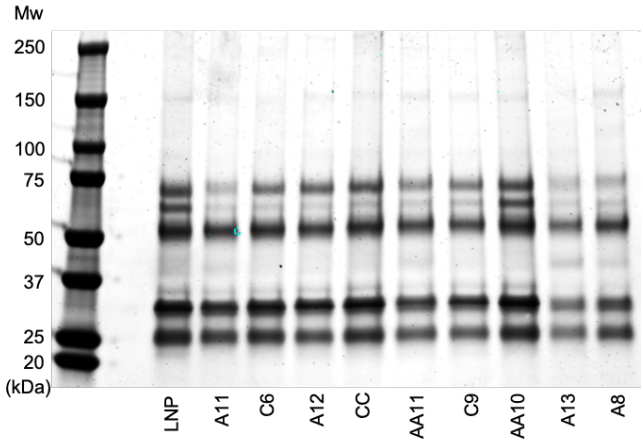

Supplementary Fig. 14 | SDS–PAGE of the plasma proteins adsorbed to the surface of mDLNP and 9 BM SORT LNPs.

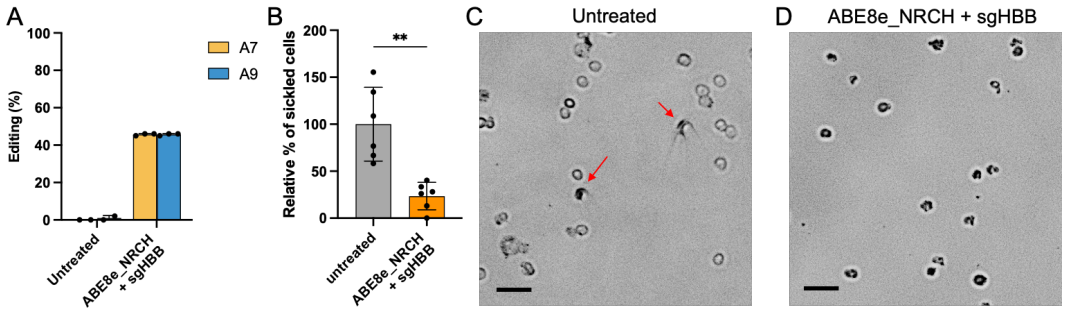

Supplementary Fig. 15 | Base editing in SCD CD117+ cells mediated by C6-LNP co-delivery of ABE8e_NRCH mRNA and sgHBB reduces sickling of differentiated erythrocytes. (A) Editing efficiencies determined by Sanger sequencing 3 days after LNP treatment. Data are presented as mean ± s.d. (n = 2 for PBS, n = 3 for base edited samples, biologically independent samples). **(B)** Base editing on CD117+ cells isolated from Townes mice reduced sickling frequency on differentiated erythrocytes. Data are presented as mean ± s.d. (n = 6 biologically independent samples). $^{**}P < 0.01$ determined by

two-tailed t-test. **(C) (D)** Representative bright field images of glutaraldehyde fixed erythrocytes differentiated from untreated or base edited CD117+ cells. Scale bar: 10 μm.

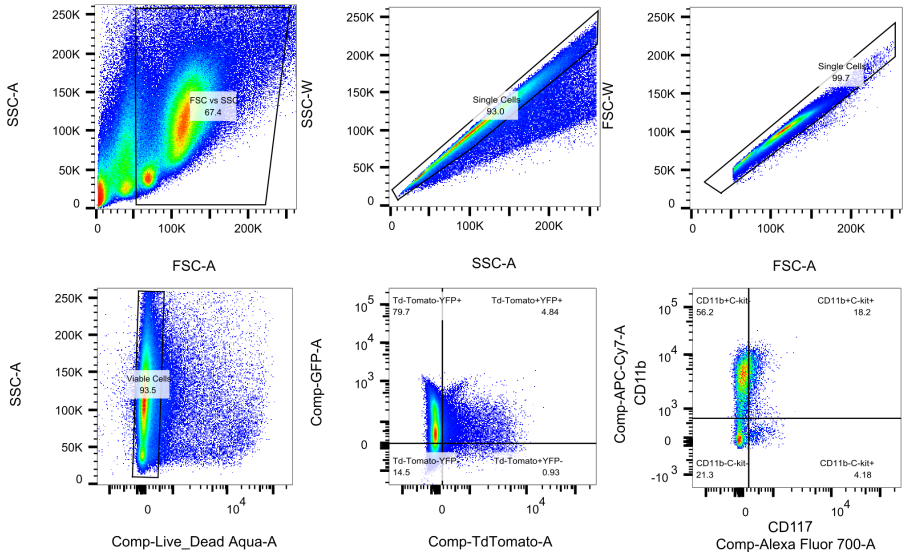

Supplementary Fig. 16 | The FACS gating strategy for analysis of tdTom+ cells in leukemic cells are presented. Live-Dead aqua was used to distinguish live cells. Leukemic cells are YFP+. CD11b and CD117 were used to distinguish leukemic stem cells.

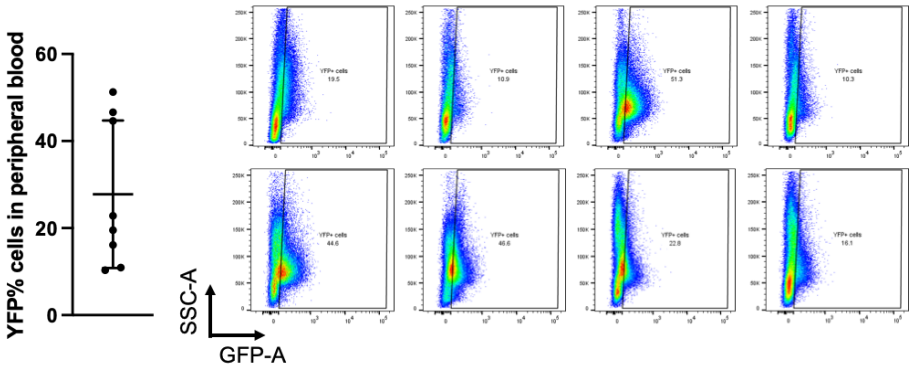

Supplementary Fig. 17 | YFP% cells in peripheral blood of recipient mice 3 weeks after transplantation of Lin- cells receiving MLL-AF9-IRES-YFP-encoding plasmid lentiviral transduction. Lin- cells were isolated from tdTom mice. A total of 8 mice received transplantation. Summary (left) and individual (right) flow cytometry analysis of peripheral blood.

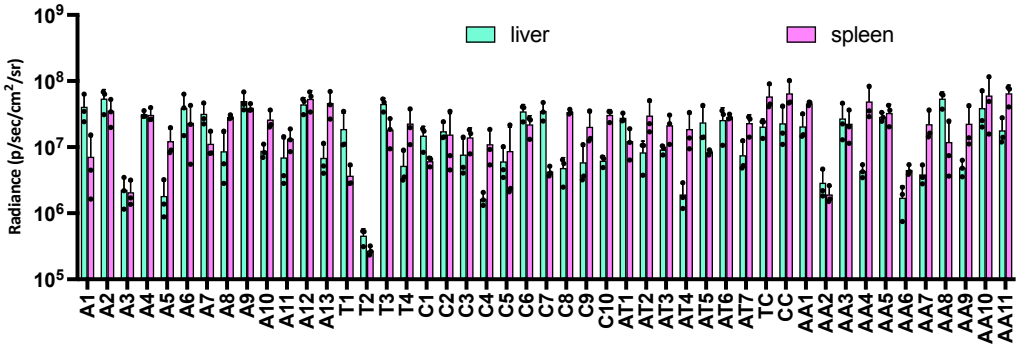

Supplementary Fig. 18 | Off-organ Luc mRNA delivery to liver and spleen by BM homing LNP formulations. Data are presented as mean ± s.d. (n = 3 biologically independent samples).

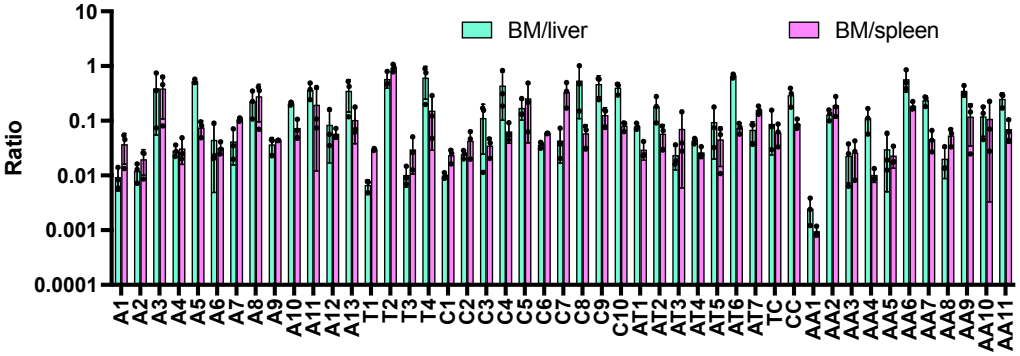

Supplementary Fig. 19 | Ratio of bone marrow bioluminescence intensity over that of liver and spleen for all tested covalent lipid species and crosslinkers. Data are presented as mean ± s.d. (n = 3 biologically independent samples).

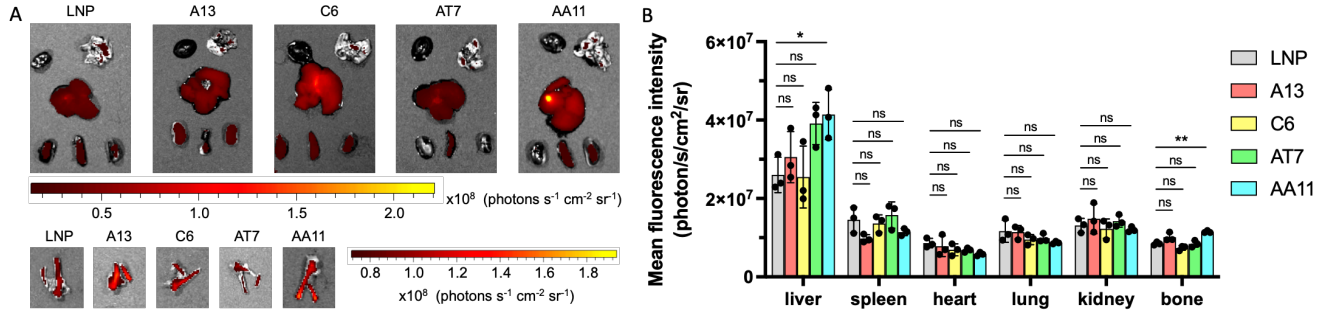

Supplementary Fig. 20 | Representative fluorescent images (A) and average fluorescent signal intensity (B) of major organs and dissected femurs. Mice received IV injection of mDLNP or BM homing LNPs containing Cy5-labeled mRNA and ex vivo imaging was conducted 2 hours after injection. Data are presented as mean ± s.d. (n = 3 biologically independent samples). ns, no significant difference, **P* < 0.05, ***P* < 0.01 determined by one-way ANOVA with multiple-comparison test.

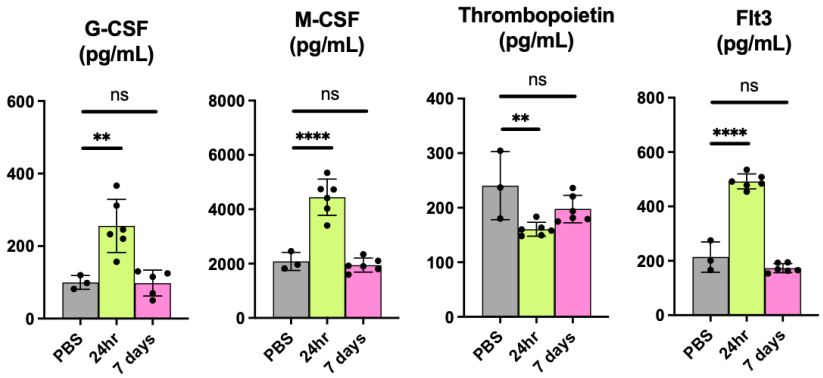

Supplementary Fig. 21 | Serum level of G-CSF, M-CSF, Thrombopoietin, and Flt3 of C57BL6 mice upon PBS and 0.6 mg/kg C6-mDLNP treatment. For LNP treated animals, serum was collected twice 24 hours and 7 days after IV injection. Data are presented as mean ± s.d. (n = 3 for PBS, n = 6 for LNP treated groups, biologically independent samples). ns, no significant difference, $^{**}P < 0.01$, $^{****}P < 0.0001$ determined by one-way ANOVA with multiple-comparison test.

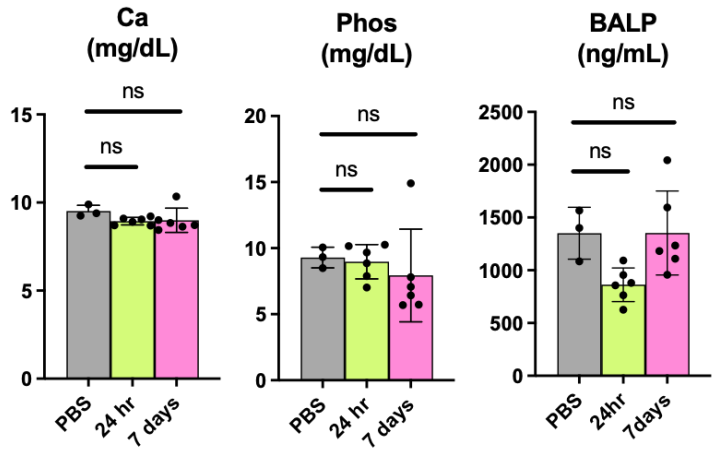

Supplementary Fig. 22 | Serum level of Ca, Phosphate (Phos) and bone-specific alkaline phosphatase (BALP) of C57BL6 mice upon PBS and 0.6 mg/kg C6-mDLNP treatment. For LNP treated animals, serum was collected twice 24 hours and 7 days after IV injection. Data are presented as mean ± s.d. (n = 3 for PBS, n = 6 for LNP treated groups, biologically independent samples). ns, no significant difference determined by one-way ANOVA with multiple-comparison test.

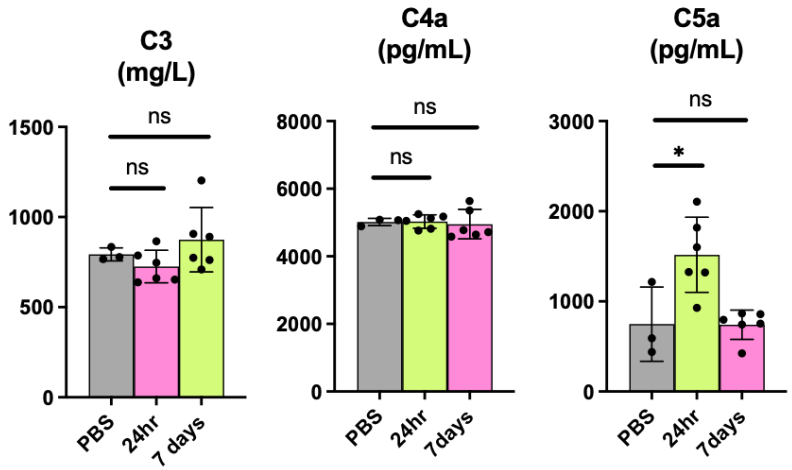

Supplementary Fig. 23 | Serum level of anaphylatoxins (C3, C4a and C5a) of C57BL6 mice upon PBS and 0.6 mg/kg C6-mDLNP treatment. For LNP treated animals, serum was collected twice 24 hours and 7 days after IV injection. Data are presented as mean ± s.d. (n = 3 for PBS, n = 6 for LNP treated groups, biologically independent samples). ns, no significant difference, *P < 0.05 determined by one-way ANOVA with multiple-comparison test.

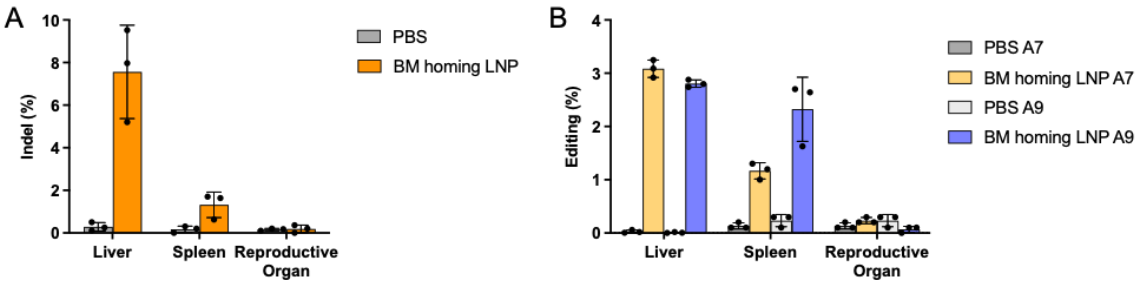

Supplementary Fig. 24 | Off-organ genomic (A) and base (B) editing in liver, spleen and reproductive organ of *HBB*$^{S/S}$ Townes mice mediated by Cas9 and ABE8e_NRCH and targeting sgRNA, respectively. Data are presented as mean ± s.d. (n = 3, biologically independent samples).

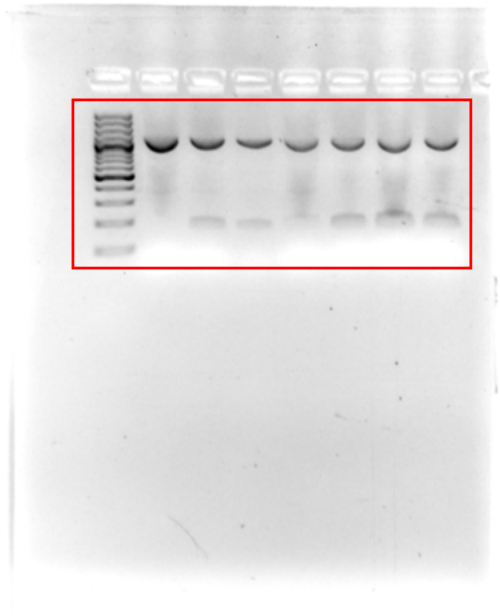

Supplementary Fig. 25 | Original gel image of Figure 5E.

Supplementary Tables

Supplementary Table 1. Summary of abbreviation, full name and cell surface marker of selected cell sub-populations.

Abbreviation	Full name	Cell surface marker
LT-HSC	long-term hematopoietic stem cell	$Lin^-Sca1^+CD117^+CD34^-CD135^-$
LMPP	lympho-myeloid primed progenitor	$Lin^-Sca1^+CD117^+CD34^-CD135^+$
MPP	multipotent progenitors	$Lin^-Sca1^+CD117^+CD34^+CD135^-$
CMP	common myeloid progenitor	$Lin^-Sca1^-CD117^+CD34^+CD16/32^-$
GMP	granulocyte-monocyte progenitor	$Lin^-Sca1^-CD117^+CD34^+CD16/32^+$
MEP	megakaryocyte-erythrocyte progenitor	$Lin^-Sca1^-CD117^+CD34^-CD16/32^-$
B	B cells	$B220^+CD3^-Ly\text{-}6G^-CD11b^-TER\text{-}119^-$
T total	T cells	$CD3^+$
T CD4	CD4+ T cells	$CD3^+CD4^+CD8^-$
T CD8	CD8+ T cells	$CD3^+CD8^+CD4^-$
Macrophage	Macrophage	$Ly\text{-}6G^-F4/80^+$
Monocyte	Monocyte	$Ly\text{-}6G^-F4/80^-$
Neutrophil	Neutrophil	$Ly\text{-}6G^+$
Leuk	Leukemia cells	YFP^+
LSC	Leukemic stem cells	$YFP^+CD11b^+CD117^+$

Supplementary Table 2. Summary of LNP formulation details mentioned in the current study.

Name	Molar Percentage (%)					
	5A2-SC8	DOPE	Cholesterol	DMG-PEG	18-PA	Covalent lipid species
LNP	23.81	23.81	47.62	4.62	0	0
Spleen SORT	19.05	19.05	38.10	3.81	20	0
BM homing LNP	19.05	19.05	38.10	3.81	0	20
C6-LNP	19.05	19.05	38.10	3.81	0	20
AA11-LNP	19.05	19.05	38.10	3.81	0	20
10% AA11	21.43	21.43	42.86	4.29	0	10
30% AA11	16.67	16.67	33.33	3.33	0	30

Supplementary Table 3. Summary of LNP hydrodynamic diameter, ζ-potential, and mRNA encapsulation efficiency.

Entry	LNP size/nm			ζ-potential/mV			Encapsulation efficiency/%		
A6	160.8	161.1	160.7	6.48	12.9	8.55	69.79	68.51	65.37
A7	139.7	137.5	140.4	-7.02	-15.6	-10	84.13	87.92	91.83
A8	152.8	155.6	153.7	-5.95	-7.16	-8.89	92.93	92.26	93.44
A9	157.7	155.9	153.8	0.146	-0.676	-1.86	92.50	92.96	85.24
A10	150.6	150.7	150.3	-1.02	-1.2	0.0821	93.52	94.10	94.74
A11	161.8	159	161.4	-21	-22	-23	75.84	79.39	78.12
A12	135.5	134.4	135.1	-23.3	-21.9	-23.8	80.95	80.48	81.03
A13	153.7	152.2	153	0.48	0.558	-0.788	76.77	76.42	76.68
C1	152.2	150.9	151.1	7.3	6.21	7.7	87.98	88.63	88.71
C5	162.8	163.7	163.3	1.71	0.304	-2.65	81.89	82.49	83.77
C7	174.8	171.9	172	-2.91	-3.19	-3.07	84.03	84.96	84.53
C8	157.4	158.5	157.9	19.4	14.2	17.5	93.53	93.54	94.15
C9	141.5	140.9	140.4	0	-2.16	-1.32	93.09	92.83	92.15
C10	128.7	129.1	126	4.13	1.24	-4.07	91.69	90.84	92.29
TC	144.1	143.5	144.5	2.95	0.381	-0.501	84.92	85.79	85.04
CC	146.5	144.1	145	8.57	7.14	6.4	83.88	82.87	82.10
AT4	152	151.6	150.4	-2.28	-0.968	-2.46	66.61	64.39	66.58
AT5	150.9	149.6	148.2	-4.82	-4.15	-3.47	86.73	87.24	87.71
AT6	139.6	135.4	136.2	-9.37	-10.7	-9.43	93.13	92.93	92.82
AT7	158.6	158.3	161.7	-0.153	-7.21	-2.12	83.82	83.83	85.02
AA10	179.9	172.8	174.8	-3.54	-3.66	-2.36	92.70	93.58	92.86
AA11	162.1	160.4	156.3	5.73	6.29	1.44	92.00	91.70	92.28

Supplementary Table 4. Average abundance and physiological function of the proteins that are most enriched in the protein corona of A12-BM-SORT formulation (n = 3).

Protein	Abundance	Functional Class
Immunoglobulin kappa constant	16.88%	Immune Protein
Complement C1q subcomponent subunit B	14.72%	Complement Protein
Complement C1q subcomponent subunit C	9.79%	Complement Protein
Apolipoprotein E	8.29%	Apolipoprotein
Ig heavy chain V region AC38 205.12	7.43%	Immune Protein
Complement C1q subcomponent subunit A	4.8%	Complement Protein
Immunoglobulin heavy constant mu	3.77%	Immune Protein
Fibrinogen gamma chain	2.95%	Coagulation Protein
Ig gamma-2B chain C region	2.64%	Immune Protein
Ig gamma-2A chain C region secreted form	2.39%	Immune Protein
Ig heavy chain V region VH558 A1/A4	2.37%	Immune Protein
Fibrinogen beta chain	2.17%	Coagulation Protein
Albumin	2.13%	Other
Ig kappa chain V19-17	2.07%	Immune Protein
Vitronectin	1.81%	Other
Ig kappa chain V-II region 26-10	1.44%	Immune Protein
Hemoglobin subunit alpha	1.15%	Other

Ig kappa chain V-V region K2 (Fragment)	0.93%	Immune Protein
Ig heavy chain V region 1-72	0.71%	Immune Protein
Plasminogen	0.67%	Coagulation Protein
Apolipoprotein D	0.65%	Apolipoprotein

Supplementary Table 5. Average abundance and physiological function of the proteins that are most enriched in the protein corona of A8-BM-SORT formulation (n = 3).

Protein	Abundance	Functional Class
Immunoglobulin kappa constant	20.39%	Immune Protein
Complement C1q subcomponent subunit B	16.61%	Complement Protein
Complement C1q subcomponent subunit C	10.57%	Complement Protein
Apolipoprotein E	9.29%	Apolipoprotein
Ig heavy chain V region AC38 205.12	7%	Immune Protein
Complement C1q subcomponent subunit A	6%	Complement Protein
Immunoglobulin heavy constant mu	2.87%	Immune Protein
Ig gamma-2B chain C region	2.73%	Immune Protein
Ig gamma-2A chain C region secreted form	2.7%	Immune Protein
Ig heavy chain V region VH558 A1/A4	2.33%	Immune Protein
Ig kappa chain V-II region 26-10	2.04%	Immune Protein
Ig kappa chain V-V region K2 (Fragment)	1.55%	Immune Protein
Albumin	1.28%	Other
Ig kappa chain V19-17	1.11%	Immune Protein
Fibrinogen gamma chain	1.1%	Coagulation Protein
Ig heavy chain V region 1-72	0.87%	Immune Protein
Fibrinogen beta chain	0.8%	Coagulation Protein
Plasminogen	0.47%	Coagulation Protein
Hemoglobin subunit alpha	0.34%	Other
Vitronectin	0.33%	Other
Apolipoprotein D	0.25%	Apolipoprotein

Supplementary Table 6. Average abundance and physiological function of the proteins that are most enriched in the protein corona of C9-BM-SORT formulation (n = 3).

Protein	Abundance	Functional Class
Apolipoprotein E	19.47%	Apolipoprotein
Complement C1q subcomponent subunit B	12.74%	Complement Protein
Immunoglobulin kappa constant	9.45%	Immune Protein
Ig heavy chain V region AC38 205.12	9.19%	Immune Protein
Complement C1q subcomponent subunit C	6.62%	Complement Protein
Immunoglobulin heavy constant mu	5.3%	Immune Protein
Complement C1q subcomponent subunit A	4.13%	Complement Protein
Vitronectin	3.87%	Other

Ig gamma-2A chain C region secreted form	3.59%	Immune Protein
Ig heavy chain V region VH558 A1/A4	3.43%	Immune Protein
Albumin	2.8%	Other
Ig gamma-2B chain C region	2.69%	Immune Protein
Ig heavy chain V region 1-72	1.1%	Immune Protein
Fibrinogen gamma chain	0.94%	Coagulation Protein
Plasminogen	0.87%	Coagulation Protein
Ig kappa chain V-II region 26-10	0.78%	Immune Protein
Apolipoprotein D	0.78%	Apolipoprotein
Fibrinogen beta chain	0.71%	Coagulation Protein
Ig kappa chain V19-17	0.62%	Immune Protein
Ig kappa chain V-V region K2 (Fragment)	0.41%	Immune Protein
Hemoglobin subunit alpha	0.11%	Other

Supplementary Table 7. Average abundance and physiological function of the proteins that are most enriched in the protein corona of AA10-BM-SORT formulation (n = 3).

Protein	Abundance	Functional Class
Apolipoprotein E	16.18%	Apolipoprotein
Immunoglobulin kappa constant	15.61%	Immune Protein
Complement C1q subcomponent subunit B	12.59%	Complement Protein
Complement C1q subcomponent subunit C	9.21%	Complement Protein
Ig heavy chain V region AC38 205.12	6.59%	Immune Protein
Complement C1q subcomponent subunit A	4.78%	Complement Protein
Immunoglobulin heavy constant mu	4.49%	Immune Protein
Ig gamma-2A chain C region secreted form	2.42%	Immune Protein
Ig heavy chain V region VH558 A1/A4	2.4%	Immune Protein
Vitronectin	2.25%	Other
Ig gamma-2B chain C region	2.13%	Immune Protein
Fibrinogen gamma chain	1.65%	Coagulation Protein
Albumin	1.59%	Other
Ig kappa chain V-II region 26-10	1.41%	Immune Protein
Apolipoprotein D	1.39%	Apolipoprotein
Fibrinogen beta chain	1.2%	Coagulation Protein
Ig kappa chain V19-17	1.19%	Immune Protein
Ig kappa chain V-V region K2 (Fragment)	0.9%	Immune Protein
Plasminogen	0.83%	Coagulation Protein
Ig heavy chain V region 1-72	0.8%	Immune Protein
Hemoglobin subunit alpha	0.15%	Other

Supplementary Table 8. Average abundance and physiological function of the proteins that are most enriched in the protein corona of A11-BM-SORT formulation (n = 3).

Protein	Abundance	Functional Class
Apolipoprotein E	17.74%	Apolipoprotein
Immunoglobulin kappa constant	16.55%	Immune Protein
Complement C1q subcomponent subunit B	13.85%	Complement Protein
Complement C1q subcomponent subunit C	9.33%	Complement Protein
Ig heavy chain V region AC38 205.12	8.89%	Immune Protein
Complement C1q subcomponent subunit A	4.5%	Complement Protein
Immunoglobulin heavy constant mu	3.84%	Immune Protein
Ig heavy chain V region VH558 A1/A4	2.97%	Immune Protein
Ig gamma-2B chain C region	2.6%	Immune Protein
Ig gamma-2A chain C region secreted form	2.6%	Immune Protein
Ig kappa chain V-II region 26-10	1.46%	Immune Protein
Ig kappa chain V19-17	1.44%	Immune Protein
Ig heavy chain V region 1-72	1.11%	Immune Protein
Vitronectin	1.03%	Other
Ig kappa chain V-V region K2 (Fragment)	0.94%	Immune Protein
Albumin	0.94%	Other
Plasminogen	0.86%	Coagulation Protein
Fibrinogen gamma chain	0.74%	Coagulation Protein
Fibrinogen beta chain	0.51%	Coagulation Protein
Apolipoprotein D	0.5%	Apolipoprotein
Hemoglobin subunit alpha	0.25%	Other

Supplementary Table 9. Average abundance and physiological function of the proteins that are most enriched in the protein corona of C5-BM-SORT formulation (n = 3).

Protein	Abundance	Functional Class
Apolipoprotein E	17.69%	Apolipoprotein
Complement C1q subcomponent subunit B	17.03%	Complement Protein
Fibrinogen beta chain	13.9%	Coagulation Protein
Apolipoprotein D	9.36%	Apolipoprotein
Hemoglobin subunit alpha	7.37%	Other
Complement C1q subcomponent subunit C	5.14%	Complement Protein
Immunoglobulin kappa constant	3.8%	Immune Protein
Fibrinogen gamma chain	3.04%	Coagulation Protein
Ig kappa chain V-V region K2 (Fragment)	2.68%	Immune Protein
Plasminogen	2.32%	Coagulation Protein
Albumin	2.29%	Other
Vitronectin	1.36%	Other
Ig heavy chain V region AC38 205.12	1.35%	Immune Protein

Immunoglobulin heavy constant mu	0.95%	Immune Protein
Ig heavy chain V region VH558 A1/A4	0.92%	Immune Protein
Complement C1q subcomponent subunit A	0.79%	Complement Protein
Ig kappa chain V-II region 26-10	0.72%	Immune Protein
Ig gamma-2B chain C region	0.62%	Immune Protein
Ig heavy chain V region 1-72	0.45%	Immune Protein
Ig kappa chain V19-17	0.3%	Immune Protein
Ig gamma-2A chain C region secreted form	0.1%	Immune Protein

Supplementary Table 10. Average abundance and physiological function of the proteins that are most enriched in the protein corona of CC-BM-SORT formulation (n = 3).

Protein	Abundance	Functional Class
Apolipoprotein E	26.18%	Apolipoprotein
Immunoglobulin kappa constant	16.25%	Immune Protein
Complement C1q subcomponent subunit B	11.05%	Complement Protein
Complement C1q subcomponent subunit C	6.52%	Complement Protein
Ig heavy chain V region AC38 205.12	6.27%	Immune Protein
Complement C1q subcomponent subunit A	4.03%	Complement Protein
Vitronectin	3.71%	Other
Immunoglobulin heavy constant mu	3%	Immune Protein
Ig heavy chain V region VH558 A1/A4	2.65%	Immune Protein
Ig gamma-2A chain C region secreted form	2.14%	Immune Protein
Ig gamma-2B chain C region	1.87%	Immune Protein
Plasminogen	1.41%	Coagulation Protein
Ig kappa chain V-II region 26-10	1.33%	Immune Protein
Apolipoprotein D	1.22%	Apolipoprotein
Albumin	1.08%	Other
Ig heavy chain V region 1-72	0.86%	Immune Protein
Ig kappa chain V19-17	0.72%	Immune Protein
Ig kappa chain V-V region K2 (Fragment)	0.63%	Immune Protein
Fibrinogen gamma chain	0.51%	Coagulation Protein
Fibrinogen beta chain	0.35%	Coagulation Protein
Hemoglobin subunit alpha	0.15%	Other

Supplementary Table 11. Average abundance and physiological function of the proteins that are most enriched in the protein corona of A13-BM-SORT formulation (n = 3).

Protein	Abundance	Functional Class
Apolipoprotein E	20.43%	Apolipoprotein
Immunoglobulin kappa constant	17.78%	Immune Protein
Complement C1q subcomponent subunit B	10.68%	Complement Protein
Ig heavy chain V region AC38 205.12	7.22%	Immune Protein

Complement C1q subcomponent subunit C	7.16%	Complement Protein
Vitronectin	4.18%	Other
Immunoglobulin heavy constant mu	4.13%	Immune Protein
Complement C1q subcomponent subunit A	3.6%	Complement Protein
Ig gamma-2A chain C region secreted form	2.46%	Immune Protein
Ig heavy chain V region VH558 A1/A4	2.34%	Immune Protein
Ig gamma-2B chain C region	2.06%	Immune Protein
Ig kappa chain V-II region 26-10	1.63%	Immune Protein
Apolipoprotein D	1.34%	Apolipoprotein
Albumin	1.19%	Other
Plasminogen	1.11%	Coagulation Protein
Ig heavy chain V region 1-72	0.88%	Immune Protein
Ig kappa chain V-V region K2 (Fragment)	0.78%	Immune Protein
Ig kappa chain V19-17	0.71%	Immune Protein
Fibrinogen gamma chain	0.55%	Coagulation Protein
Fibrinogen beta chain	0.4%	Coagulation Protein
Hemoglobin subunit alpha	0.19%	Other

Supplementary Table 12. Average abundance and physiological function of the proteins that are most enriched in the protein corona of AA11-BM-SORT formulation (n = 3).

Protein	Abundance	Functional Class
Apolipoprotein E	23.58%	Apolipoprotein
Immunoglobulin kappa constant	19.32%	Immune Protein
Complement C1q subcomponent subunit B	10.68%	Complement Protein
Complement C1q subcomponent subunit C	6.95%	Complement Protein
Ig heavy chain V region AC38 205.12	5.75%	Immune Protein
Albumin	4.94%	Other
Complement C1q subcomponent subunit A	3.68%	Complement Protein
Immunoglobulin heavy constant mu	2.6%	Immune Protein
Ig heavy chain V region VH558 A1/A4	2.28%	Immune Protein
Vitronectin	2.27%	Other
Ig gamma-2A chain C region secreted form	2.04%	Immune Protein
Ig gamma-2B chain C region	1.72%	Immune Protein
Ig kappa chain V-II region 26-10	1.3%	Immune Protein
Plasminogen	1.29%	Coagulation Protein
Apolipoprotein D	1.14%	Apolipoprotein
Ig kappa chain V19-17	0.68%	Immune Protein
Ig heavy chain V region 1-72	0.64%	Immune Protein
Ig kappa chain V-V region K2 (Fragment)	0.58%	Immune Protein
Fibrinogen gamma chain	0.45%	Coagulation Protein
Fibrinogen beta chain	0.3%	Coagulation Protein

Hemoglobin subunit alpha	0.2%	Other

Supplementary Table 13. Average abundance and physiological function of the proteins that are most enriched in the protein corona of mDLNP formulation (n = 3).

Protein	Abundance	Functional Class
Apolipoprotein E	22.1%	Apolipoprotein
Immunoglobulin kappa constant	18.39%	Immune Protein
Complement C1q subcomponent subunit B	9.86%	Complement Protein
Ig heavy chain V region AC38 205.12	7.5%	Immune Protein
Complement C1q subcomponent subunit C	6.7%	Complement Protein
Albumin	3.92%	Other
Vitronectin	3.61%	Other
Complement C1q subcomponent subunit A	3.31%	Complement Protein
Immunoglobulin heavy constant mu	3.04%	Immune Protein
Ig gamma-2A chain C region secreted form	2.28%	Immune Protein
Ig heavy chain V region VH558 A1/A4	2.25%	Immune Protein
Ig gamma-2B chain C region	2.14%	Immune Protein
Ig kappa chain V-II region 26-10	1.66%	Immune Protein
Plasminogen	1.25%	Coagulation Protein
Apolipoprotein D	1.18%	Apolipoprotein
Ig heavy chain V region 1-72	0.79%	Immune Protein
Ig kappa chain V19-17	0.72%	Immune Protein
Ig kappa chain V-V region K2 (Fragment)	0.67%	Immune Protein
Fibrinogen gamma chain	0.47%	Coagulation Protein
Fibrinogen beta chain	0.35%	Coagulation Protein
Hemoglobin subunit alpha	0.2%	Other

Supplementary Table 14. The protospacer sequences of sgRNAs used in this study. All sgRNAs have 3X 2'-O-methyl phosphorothioate (MS) modification on both 5’ and 3’ ends.

Name	Sequence (5' to 3')	PAM (5' to 3')
sgHBB	TTCTCCACAGGAGTCAGGTG	CACC
sgG34	CTTGTCAAGGCTATTGGTCA	AGG

Supplementary Table 15. Forward and reverse primers of PCR products.

Name	Forward Primer (5' to 3')	Reverse Primer (5' to 3')
Luc	GCAACCTCAAACAGACACCGCCACCATG GAAGACGCCAAAAACAT	TGGACAGCAAGAAAGCGAGCTTACACGG CGATCTTTCCGC
NLS-Cre	GCAACCTCAAACAGACACCGCCACCATG CCCAAGAAGAAGAGGAA	TGGACAGCAAGAAAGCGAGCTTAATCGC CATCTTCCAGCAGG

NLS-Cas9-SV40 NLS-Nucleoplasmin NLS	GCAACCTCAAACAGACACCGCCACCATG CGCGCCGCTCCGGCAGCTAA	TGGACAGCAAGAAAGCGAGCTCACTTTT TCTTTTTTGCCTGGCCGGCC
SV40 NLS-ABE8e_NRCH-SV40 NLS	GCAACCTCAAACAGACACCGCCACCATG GCCCCAAAGAAGAAGCGG	TGGACAGCAAGAAAGCGAGCTTAGACTT TCCTCTTCTTCTTGGGC
Ai14	GCTCCTGGGCAACGTGCTGG	TGCAGGTCGAGGGACCTAATAACTT

Supplementary Table 16. Forward and reverse primers of PCR products used for NGS.

Name	Forward Primer (5' to 3')	Reverse Primer (5' to 3')
HBG1	ATTCTTCATCCCTAGCCAGCCGC	TGACTGAATCGGAACAAGGCAAAGG
HBB	GCCACACCCTAGGGTTG	GGGAAAATAGACCAATAGGCAG